Doctoral Dissertation

Marine Ecosystem Variations and Predictability of Sea Surface Temperature in the North Pacific

(北太平洋における海洋生態系の変動と海洋表面水温の予測可能性)

Emi Yati

Graduate School of Science, Hokkaido University

Department of Natural History Science

2020 September

Abstract

Monitoring climatic parameters and their biological effect across various time scales has important economic and ecological implications. This dissertation describes marine ecosystem variability and its relation to large-climate variability and change and sea surface temperature (SST) predictability over the North Pacific (NP) from the latest seasonal forecast systems.

Time series data for 120 marine species of zooplankton, invertebrates, small-pelagic fish, groundfish, and salmon in both the eastern and western NP basins and eight physical (climate) indices were analyzed by a large multivariate analysis to identify dominant modes of marine ecosystem variability and their relation to physical climate in 1965–2006. An empirical orthogonal function (EOF) of marine biology was performed. The time series of the first EOF mode (PC1) of marine biology for the eastern, western and the whole NP are characterized by a long-term trend in 1978-1998, accompanied by a decrease in groundfish and the increase in salmon in both basins as well as an increase of most of small pelagic fishes in the western NP and decrease zooplankton in the eastern NP. The time series of the second mode (PC2) of eastern NP marine biology exhibited multi-decadal variability with two phase reversals, while the western NP marine biology PC2 exhibited interdecadal variability with three phase reversals. All of marine biology PC1s were correlated with the SST anomalies (SSTs) averaged over the NP and with the globally averaged SSTs, suggesting that the leading mode of the marine ecosystem variations may influence by global warming. The eastern NP PC2 was the most strongly correlated with the Pacific Decadal Oscillation (PDO),

while the western NP marine biology PC2 was correlated with the North Pacific Gyre Oscillation (NPGO).

In an investigation of SST predictability, prediction skills and their association with the relations among ensemble members and observation were analyzed for January and July forecasts with 3-month lead time by using 95 members of multi-model ensemble in 1994-2016. The seasonal forecast system which produced by the European Centre for Medium-Range Weather Forecasts (ECMWF), Deutscher Wetterdienst (DWD), and Centro-Euro-Mediterraneo Sui Cambiamenti Climatici (CMCC) were used and the data were downloaded from the Copernicus Climate Change Service (C3S). The prediction skill was estimated using the temporal correlation between the multi-model ensemble mean (MMEM) and observed SSTs at each grid point, referred to as point-wise correlation. These point-wise correlations were high in the eastern and central NP in January and in the eastern NP in July and were low in the Kuroshio-Oyashio Extensions (KOE) in both January and July and in the central NP in July. Further analysis revealed that areas with high prediction skill show small spreads among ensemble members and that an observation can be regarded as an ensemble member. Low prediction skill was associated with either a large ensemble spread as found for the July KOE, or the failure of ensemble members to capture observed variability, as found in the January KOE and in the July central NP. The former case was associated with predictable component relative to stochastic component, and the latter case is resulted from biased variations commonly occurred across ensemble members.

Table of Contents

Chapter 1

General Introduction

The effects of climate variability on interannual to decadal time scales and anthropogenic climate change, especially global warming, on marine ecosystems have been extensively studied (e.g., Hare and Mantua 2000; and Poloczanska et al. 2016), because marine ecosystem change can impact on fisheries and socioeconomic (Sumaila et al. 2011). A key variable linking climate to marine ecosystem is sea surface temperature (SST), because SST is one of physical forcing on marine ecosystem variation (Tommasi et al. 2017; Hobday et al 2018). SST is also used in climate models to predict climate phenomena on interannual to decadal time scales, such as EL Niño Southern Oscillation (ENSO) (e.g., Johnson et al. 2019), Pacific Decadal Oscillation (PDO) (Mantua et al. 1997) and global warming (e.g., Bindoff et al. 2019). Therefore, understanding marine ecosystem variation and SST predictability in climate models is important. In this research, marine ecosystem variations and SST predictability in the North Pacific (NP) are examined.

A useful approach to understand marine ecosystem variation in a more holistic view, than analyses of selected species, is to analyze a large number of marine biological indices by using a multivariate analysis method. This approach has been employed for California waters, Gulf of Alaska to the Bering Sea (Hare and Mantua 2000; Litzow and Mueter 2014) and the Sea of Japan (Tian et al. 2006) and the Yellow and East China Seas (Ma et al. 2019), however, it has not been applied to the whole NP (i.e., California waters , the Gulf of Alaska, the Bering Sea and the Sea of Okhotsk to the Sea of Japan). The influence of large-scale climate variability on marine ecosystems from California

waters to the Bering Seas (Hare and Mantua 2000; Litzow and Mueter 2014) and the Sea of Japan (Tian et al. 2006) has been reported. Therefore, in Chapter 2, marine ecosystem variations in the whole NP and its relation to large scale climate variability and anthropogenic climate change, especially global warming, are investigated.

SST, one of the oceanic variables that plays an important role in climate variability and change, is a target variable of seasonal (i.e., one to 12 months) forecast conducted by many climate centers. The utilize of Multi Model Ensemble (MME) technique (Becker et al. 2014; Kirtman et al. 2014) from the seasonal forecast has been considered as effective way to provide the prediction at representing SST variation. Related to the seasonal forecast which produced by a coupled climate model, Copernicus Climate Change Services (C3S) in Europe, recently provides the operational data from five climate centers in Europe and one center in the United State (Min et al. 2020). Therefore, in Chapter 3, the SST predictability in MME of C3S was analyzed. The North Pacific is used as a study area in Chapter 3 as in Chapter 2.

The knowledge of the climate and marine ecosystem co-variability in Chapter 2 and the information of the seasonal SST predictability in climate forecasting systems in Chapter 3 suggest that the seasonal forecast model can be used for possible prediction of marine ecosystem variation, but cannot be directly used because of the discrepancy in the time scale, as explained in Chapter 4.

Chapter 2

Marine Ecosystem Variations in the North Pacific and Its Relation to Large-Scale Climate Variability and Change

2.1. Introduction

Marine ecosystem is influenced by climate variability and change. Unlike natural climate variability, climate change generally results from anthropogenic changes. The effect of physical climate variability on marine species in the North Pacific (NP) has been studied in the last few decades. Earlier studies focused their attention on relatively limited numbers of marine species such as salmon (Beamish and Bouillon 1993; Francis and Hare 1994; Mantua et al. 1997; Beamish et al. 1999; Hare et al. 1999) and sardine (Kawasaki and Omori 1995; Noto and Yasuda 1999; Yasuda et al. 1999). An important finding of these studies is that large-scale decadal variability of climate characterized by Aleutian Low strength changes and associated sea-surface temperature (SST) anomalies, which is known as Pacific (inter-)Decadal Oscillation (PDO; Mantua et al. 1997; Minobe 1997), has a substantial influences marine species (e.g., Mantua et al. 1997; Beamish et al. 1997).

As an evidence of climate influence on marine ecosystem, step-like shifts commonly occurring in both the marine ecosystem indices and physical climate attracted attentions (Ebbesmeyer et al. 1991), such a shift is often referred as a regime shift. A regime shift for physical climate is defined as a transition from one climatic

state to another within a period substantially shorter than the lengths of the individual epochs of each climate state (Minobe 1997). A regime shift for marine ecosystem can also be defined in the same way as the climatic regime shift, i.e., a rapid change on multidecadal time scales (Möllmann and Diekmann 2012); however, sometimes marine ecosystem regimes mean different states of dominant species (e.g., Lluch-Belda et al. 1989). In this dissertation, the marine ecosystem regime shift in the former meaning, (i.e., a rapid step-like change) is used.

To understand the marine ecosystem variability and change in a more wholistic way compared with analyses of selected species, a useful approach is an analysis of a large number of marine biological indices by using a multivariate analysis method. This type of analysis is called Large number Multivate Analysis (LMA). The pioneering first study of LMA is conducted by Hare and Mantua (2000), who analyzed 69 marine species time series data in the eastern NP (i.e., from California waters to the Bering Sea) combined with 31 physical climate indices from 1965 to 1997. They applied an Empirical Orthogonal Function (EOF) analysis, which is the same as principal component analysis in general statistics. They reported that regime shifts occurred in 1976/1977 and 1988/1989 in marine ecosystem over the eastern NP. A decade later, by using 64 eastern NP biological time series with several climate indices in 1965-2008, Litzow and Mueter (2014) also reported shifts in marine biology in the 1976/1977 but they did not find biological shift in the late 1980s. Rather, they emphasized that the time series of the first biological EOF1 is characterized by a gradual change and not by a step-like shift. Focusing on the western side of NP basin, Tian et al. (2006) analyzed 58 Japanese fish catch data in the Sea of Japan in 1958-2003, and Ma et al. (2019) recently analyzed 147 catch data in the Yellow and East China Seas in 1965-2008. Tian et al.

(2006) reported that the biological EOF1 mode is highly correlated with PDO (Mantua et al. 1997) and the Arctic Oscillation (AO) (Thompson and Wallace 1998), while Ma et al. (2019) found strong correlations between biological PCs with local physical condition but not with large scale climate modes.

It should be noted that previous LMA studies are limited either in the eastern basin only or marginal seas in the western NP (the Sea of Japan, the Yellow and East China Seas) only. This hinders us from understanding of the marine ecosystem variability and change over the whole NP in a unified manner. It is already known that climate variability causes changes in marine ecosystem in the eastern and western side of the NP for sardine and anchovy (Lluch-Belda et al. 1992; Kawasaki and Omori 1995; Yasuda et al. 1999; Chavez et al. 2003) and for salmon (e.g., Beamish and Bouillon 1993). These results underline the importance of the whole basin analyses.

Therefore, the purpose of this study is to identify the important modes of marine ecosystem variations in the last half century both in the western and eastern NP basin and their relations to basin-scale physical climate variability and change. To this end, 120 marine species time series, consisting of 91 eastern NP and 29 western NP time series were analyzed. The marine species time series were consisting of zooplankton, invertebrates, small-pelagic fish, groundfish and salmon. This is the first LMA study analyzing data from both western and eastern NP basins. EOF analysis on biological data were applied to identify important modes, and correlation analysis was used to understand the relationships between marine ecosystem and physical climate. In addition to climate variability (such as PDO and North Pacific Gyre Oscillation (NPGO) (Di Lorenzo et al. 2013)), the NP-averaged and global-averaged SST time

series, which were not examined by the previous LMA studies, were analyzed to clarify the possible relation between marine ecosystem changes and global warming.

2. 2. Data and Methods

A total of 120 annual marine biological samples (Table 2.1), consisting of 29 data for the western NP time series from Japan and Russia, and 91 for the eastern NP over areas of the Bering Sea, the Gulf of Alaska and the West coast of United States were used. The time series consist of 54 groundfish recruitments, 13 small-pelagic recruitments, 34 salmon abundance, 8 invertebrate recruitments, and 11 zooplankton biomasses. Some of our eastern NP data are overlapped with those used by previous studies; 48% of groundfish, 80% of small-pelagic, 13 % of invertebrate and 25 % of salmon were also used by Litzow and Mueter (2014). On the other hand, western NP data analyzed in the present study have not been used for previous LMA studies, because previous studies of the western NP used catch data. The analysis period was 1965 to 2006 based on a criteria of available data ratio exceeding 50%, as in Hare and Mantua (2000). This period was 10 years longer than the analysis period of Hare and Mantua (2000), but similar to that of Litzow and Mueter (2014). Some of the results are shown by map-format for NP basin and the correspondences between the index number along with abbreviation shown in Table 2.1 and spatial position on the map are summarized in Figure 2.1.

To determine the relationship between variation in marine ecosystems and climate, eight physical climate indices were used , which are annually-averaged global sea-surface temperature anomalies (SSTA), NP SSTA, PDO, NPGO, multivariate El

Niño-Southern Oscillation Index (MEI) (Wolter and Timlin 2011), Aleutian-low pressure index (ALPI) (Beamish et al. 1997), North Pacific Index (NPI) (Trenberth and Hurrell 1994) and AO (Table 2.2). Both the ALPI and NPI represent the strength of the Aleutian Low, a large-scale low-pressure over the North Pacific in winter. Its strength is closely related to the PDO. The SST dataset used in present study, including the calculation of SSTA indices was Centennial in Situ Observation-Based Estimates of the Variability of SST and Marine Meteorological Variables (COBE) version 2 (Hirahara et al. 2014).

The EOF technique was employed to analyze the marine biological indicators, and EOF modes were calculated separately for the whole, western, and eastern NP indicators. Before calculating the EOF, marine biological indicators were normalized. Thus, reflecting the larger number of time series in the eastern NP than in the western NP, the former more strongly contributes to the whole NP EOF than the latter does. The covariance between the two biological time series was calculated for the temporal points at which data were available for both time series (von Storch and Zwiers 2012). The relation between the EOF time series and respective biological or physical time series were evaluated by the Pearson's correlation coefficients. Because co-variability among biological indicators mostly occur on decadal time scales, 5-year running means were applied for marine biology time series figures.

The Statistical significance of the correlation was estimated by using a Monte-Carlo simulation. First, a surrogate 1,000 time series for the respective PCs was generated using a red noise model, where the lag-1 correlation was estimated by using Burg's method. Then surrogate correlation coefficients are calculated between observed data (e.g., marine biological indicators) and the surrogate PC time series. The

confidence level was estimated as the percentile of the absolute value of the observed correlation with respect to the surrogate correlations

2.3. Results

2.3.1 EOF Modes of Marine Biology Indices

Explained variance of the first EOF for the whole NP marine biology is 38.6%, the eastern NP marine biology is 33.5% and western NP marine biology is 46.4%. Meanwhile explained variance of the second EOF for whole NP marine biology is 26.8%, eastern NP marine biology is 28.5% and western NP marine biology is 21.7%.

Figure 2.2(a) shows the PC1s for the whole, eastern, and western NP basins. All marine biology PC1s showed a multi-decadal trend-like feature with a single-phase reversal in the 1980s, and western and eastern NP marine biology PC1s were generally similar (r=0.90), especially after 1990. The trend-like feature was consistent with the marine biology PC1s of the previous eastern NP LMAs by Hare and Mantua (2000) and Litzow and Mueter (2014) as well as the marine biology PC1s of western NP LMAs by Tian et al. (2006) and Ma et al. (2019). Interestingly, the 1980s phase reversal was gradual for the eastern NP marine biology PC1, consistent with these previous studies, but was more rapid in the western NP marine biology PC1. As expected, the whole NP marine biology PC1 shared the features of the eastern and western NP marine biology PC1s.

Figure 2.2(b,c) summarize statistically significant correlations at a confidence level of 90% between the marine biology PC1s and biological data. For the respective

basin marine biology PC1s, significant positive correlations, which mean overall increases associated with the positive trend of the marine biology PC1s, were found for 11 salmon data (32% of all salmon data) both in the western and eastern basins. Those salmon data consist of chum salmon (77.S, 83.S, and 107.S), pink salmon (82.S, 91.S, 94.S, 106.S, and 109.S), and sockeye salmon (87.S, 93.S, and 108.S) data. Here, the numbers indicate the sample IDs shown in Table 2.1. Those salmon data are mainly around the Gulf of Alaska (82.S, 83S, 87.S, 91.S, 93.S, and 94.S), the Okhotsk Sea (106.S, 107.S, and 108.S) and the Sea of Japan (109.S). Additionally, the western NP PC1s were positively correlated with half of the small-pelagic fish's data around the Sea of Japan, including the jack mackerel (74.P and 67.P) and anchovy (73.P and 68.P). Significant negative correlations with marine biology PC1s were detected for 12 groundfish data (22% of all groundfish data) across the basin, including the west coast rockfish data (09.G, 12.G, 13.G, 20.G, and 21.G), walleye pollock data (34.G, 54.G, and 63.G), cod data (35.G, 58.G, and 60.G), and others (57.G and 61.G). Significant negative correlations were detected between marine biology data and PC1s occur for one zooplankton data in the California waters (113.Z), two zooplankton data (114.Z and 115.Z) and one invertebrate data (41.I) in the Bering Sea. There were minor exceptions, including negative correlations for salmon (89.S) and small pelagic fish data (64.P and 40.P) and positive correlations of groundfish data (22.G, 27.G, and 50.S) and Jellyfish data (120.Z). Consequently, the increasing trend in marine biological PC1s were related to Alaskan and Japanese/Russia salmon abundance and some Japanese small pelagic fish recruitment increased while groundfish recruitment in both the western and the eastern NP, and zooplankton biomass in the eastern NP decreased.

Figure 2.3 shows the time series comparison between the western and eastern NP marine biology PC1s and salmon and groundfish time series in the respective basins and western NP small pelagic fishes with the 5-year running averages. It is interesting to note that the time series of the western NP salmon exhibited a rapid negative-to-positive phase transition around 1990, which appears consistent with the aforementioned rapid phase reversal of the western NP marine biology PC1. The rapid transition was not clearly seen in other western NP biological data except for Japan Pacific coast jack mackerel (P.74), and in eastern NP biological data.

Figure 2.4(a) shows the marine biology PC2s of eastern and western basins. The eastern NP marine biology PC2 was characterized by multidecadal variability with reversal phase in the 1970s and in the 1990s. The western NP marine biology PC2 exhibited three reversal phase and was characterized by interdecadal variability, shorter than that of the eastern NP marine biology PC2. The whole marine biology PC2 show similar features with eastern NP marine biology PC2 (not shown). It is noteworthy that the EOF analysis based on detrended data (i.e., removing the linear trend from marine biology data before calculating PCs), detrended marine biology PC1s (not shown) and non-detrended marine biology PC2s showed high correlation for the eastern NP (i.e., 0.93) and for the western marine biology NP (i.e., 0.83). These result support the robustness of marine biology PC2s for the respective basin.

Figure 2.4(b,c) show the statistically significant correlation coefficients for marine biology data with the respective basin marine biology PC2s. For the western basin, significant correlations were mostly negative, including correlations for salmon (102.S), small pelagic fish (65.P and 66.P) and zooplankton (119Z) data. Significant correlations for the eastern NP marine biology PC2 were positive mainly for salmon

data in the California waters (76.S), Gulf of Alaska (81.S, 84.S, 90.S, 92.S, and 95.S) and the Bering Sea (99.S). On the other hand, significant correlations for the eastern NP marine biology PC2 were negative mainly for groundfish data in the California waters (01.G, 02.G,06.G,7.G, 08.G, 10.G, 11.G, 17.G, 19.G, and 24.G), in the Gulf of Alaska (28.G, 30.G 32.G) and in the Bering Sea (51.G, 52.G). Significant negative correlations were also detected between the eastern NP PC2 with the Bering Sea Jellyfish data (120.Z), the California waters zooplankton data (110.Z) and with one invertebrate data in the Bering Sea (42.I).

Time series comparison between the eastern NP marine biology PC2 and salmon and groundfish species, that are significantly correlated with the marine biology PC2, showed positive anomalies at the end of the 1990s for most of groundfish data, but not for salmons (Figure 2.5). It is apparent that the positive anomalies at the end of the 1990s occurs for many groundfish, similar to the negative peak of eastern NP marine biology PC2 in the 1990s.

2.3.2. Relation Between Marine Biology EOFs and Climate Indices

The relationship between EOFs documented in the previous section and physical climate variability and anthropogenic climate change were further evaluated. Table 2.3 shows correlations between the PCs of marine biology and climate data. The whole NP marine biology PC1 is highly correlated with NP SSTA and with global-mean SSTA but is not significantly correlated with other climate indices (Table 2.3). Figure 2.6(a) shows that these SSTA time series share multidecadal variability with marine biology PC1s including the negative-to-positive polarity change in the 1980s. This suggests that

the warming over the NP associated with global warming may contribute to the leading mode of the NP marine biology.

The eastern NP marine biology PC2 was the strongly correlated with PDO (Table 2.3). Consistent with the strong correlation between eastern NP marine biology PC2 and the PDO index, the correlation between eastern NP marine biology with SST show similar pattern to PDO time series (Figure 2.6(b)). Both time series shared the reversal phase in the 1970s and 1990s, consistent with previously reported regime shifts (Mantua et al. 1997; Minobe 1997; Chavez et al. 2003). However, the difference between the two-time series occurred around 1990 associated with a brief negative period for the PDO without a similar feature in the eastern NP marine biology PC2. Some studies have referred that PDO phase transition in the late 1980s as a climatic regime shift (Yasunaka and Hanawa 2002); however, Minobe (2000) suggested that this was a minor regime shift and was different from the major regime shifts in the 1920s, 1940s and 1970s. The eastern NP marine biology PC2 seem did not influenced by this minor event.

In contrast to the relation between eastern NP PC2 and PDO, the western NP PC2 was correlated with NPGO (Table 2.3). It is noteworthy that there was no correlation between eastern NP PC2 and NPGO or between western NP PC2 and PDO. Based on the time series comparison, the coherent variability between the NPGO and western NP PC2 is limited in the 1990s and 2000s (Figure 2.6(c)). This may be related to the recent enhancement of decadal variability of NPGO (Di Lorenzo et al. 2013; Joh and Di Lorenzo 2017).

Figure 2.7 shows that the SST correlation patterns associated with marine biology PCs are consistent with the time series of physic climate summarized in Figure 2.6. The correlation map for the whole NP marine biology PC1 was characterized by overall positive correlations, accompanied by particularly strong correlations in the western subtropical gyre and in the East China Sea. The correlations maps with the eastern NP marine biology PC2 and with the western NP marine biology PC2 were consistent with the PDO pattern and the Victoria pattern (Bond et al. 2013), respectively. The Victoria pattern is closely related to the NPGO. For the eastern NP PC2, correlations were positive in the eastern NP and negative in the central NP, accompanied by weakly negative correlation in the western NP west of 150°E, consistent with the PDO pattern (Mantua et al. 1997). The correlations with the western NP marine biology PC2 were positive in the subtropical western NP, while the areas of negative correlations in the eastern NP were smaller than those in the Victoria pattern (Bond et al. 2013).

2.4. Summary and Discussion

The LMA of marine biology time series for both the western and eastern NP basis was conducted. Marine biology PC1s in both the eastern and western NP exhibited long-term trend in 1978-1998 and were associated with overall increases in Alaskan and Japanese/Russian salmon abundance and some small pelagic fish recruitment in the western NP and decrease of groundfish recruitment across the basin and eastern NP zooplankton biomass (Figures 2.2 and 2.3). This mode is closely related to NP-averaged and global averaged SSTs (Figures 2.2(a) and 2.6(a)). These results suggest that the

leading mode of the NP marine biology is likely influenced by global warming. The marine biology PC1s are consistent with marine biology PC1s obtained by previous studies for the eastern NP (Hare and Mantua 2000; Litzow and Mueter 2014) and with those for the western NP (Tian et al. 2006; Ma et al. 2019), although these previous studies did not examined the relation with global warming. The eastern NP marine biology PC2 characterized by multi decadal variability related to PDO (Figures 2.4(a) and 2.6(b)), whereas the western NP PC2 exhibited slightly shorter interdecadal time scales related to NPGO (Figures 2.4(a) and 2.6(c)). The eastern NP PC2 was similar to that found by Litzow and Mueter (2014); however, the western NP PC2 was different from those reported by Tian et al. (2006) for the Sea of Japan and by Ma et al. (2019) for the Yellow Sea and the East China Sea. A possible reason for the difference in the western NP PC2s between the present study and previous studies may be explained by the different spatial domains among studies. Overall, the present LMA provides an overview of variation in marine ecosystems across the western and eastern NP and marine ecosystems relation to climate variability and change.

The influence of PDO on NP marine biology PC2 and NPGO on western NP marine biology PC2 are consistent with the results of Di Lorenzo et al. (2013). Di Lorenzo et al. (2013) reported that the different climate mode have impact the long-term change in zooplankton species distribution in the Kuroshio-Oyashio Extension and California waters. As important fish food, the long-term changes zooplankton species in eastern and western NP will impact the long-term variability of higher fish trophic levels.

The marine ecosystems variation documented in this study, especially for the first EOF modes, may be related to global warming. A temperature increase due to

global warming is expected to cause the migration of marine species to colder areas, i.e., higher latitudes and deeper depths, and shifts of phenology (e.g., Pinsky et al. 2013; see also review by Poloczanska et al. 2016). This migration increases warm water species and decreases cold water species in each region, consistent with the correlation pattern between marine biology PC1s and small pelagic fishes. The correlation pattern between marine biology PC1s and small pelagic fishes were characterized by increases in jack mackerel and anchovies (P.67, P.68, P.73, P.74) and decreases in sardines (P.64) in the western NP based on the Japanese records. Migration can be more difficult for groundfish than for pelagic fishes, because demersal fish habitats can be constrained by bottom topography (Li et al. 2019). This might partly explain why a decline in groundfish is generally associated with the EOF1s across the basin. The increase in salmon mainly on the Pacific side of Alaska and Russia, is likely due to the increase in salmon hatchery in the late 20th century in these areas. Indeed, Kaeriyama et al. (2014) suggested that the increase of salmon in the second half of the 20th century was caused by global warming via the enhanced growth of age 1-year-old salmon in the Okhotsk Sea. Pacific salmon have increases on the Arctic side of the Alaska since the 1990s (Carothers et al. 2019). Therefore, earlier global warming may have provided better conditions for some Russian and Alaskan salmon, though further temperature increases can be harmful even for these species.

Of course, the climate change influences marine ecosystems not only through the temperature increases, but also via the ocean acidification and the ocean deoxygenation. Among these two threats, the species investigated in this present study may be more strongly influenced by the ocean deoxygenation. Ocean acidification threatens primarily the species that build calcium carbonate-based shells and other

structures. In the North Pacific, strong ocean deoxygenation has been observed over the last 50-60 years (Ito et al. 2017) and thus the deoxygenation may have negative effects, especially for groundfish. Indeed, Ono et al. (2011) suggested that the shoaling of the hypoxia upper boundary influences the deepest habitat of the Pacific cod over the Pacific continental shelf off northeastern coast of Japan. Ocean deoxygenation is generally caused by the increased water temperature via a reduced oxygen saturation concentration at the surface and weakened dissolved oxygen at depth water. The strong oxygen decrease over the NP may be due to the warming in the Okhotsk Sea (Nakanowatari et al. 2007). In addition, fluctuation in isopycnal surfaces and advection on the surfaces contributes to variation in dissolved oxygen concentration in regions over the NP (Pozo Buil and Di Lorenzo 2017; Ito et al. 2019). Further studies are necessary to understand the mechanisms underlying deoxygenation over NP basin and its influences on marine ecosystems.

Based on these potential mechanisms, adjustment to global warming may be more difficult for groundfish than for pelagic fishes. To further understand this comparison, the depth ranges of the fish species that have significant correlations with the biological PC1s (Figure 2.8). For EOF1, among 19 marine biology data of significant positive correlations 14 marine biology data are for species with depth range shallower than 300 m, while among 20 marine biology data of significant negative correlations 14 marine biology data are for species with depth range deeper than 300 m. These results confirm that responses generally differ between shallow and deep-water species.

Table 2.1. Summary of time series data for 120 marine species. Depth ranges (m) are those reported for juveniles and adults (but not larvae), from the shallowest to the deepest.

ID	Abbreviation	Species Name	Variable	Species	Depth range (m)	Reference of Depth range
01	SCACABZN	Southern California cabezon	Recruitment	Groundfish	0-200	Eschemeyer et al. 1983; Froese and Pauly 2019
02	CALINGCD	California lingcod	Recruitment	Groundfish	0-475	Allen and Smith 1988; Froese and Pauly 2019
03	NCACABZN	Northern California cabezon	Recruitment	Groundfish	0-200	Eschemeyer et al. 1983; Froese and Pauly 2019
04	OCBROCK	Oregon & California black rockfish	Recruitment	Groundfish	0-366	Hart 1973; Froese and Pauly 2019
05	ORKELPGLG	Oregon kelp greenling	Recruitment	Groundfish	0-200	Eschemeyer et al. 1983; Froese and Pauly 2019
06	ORCABZN	Oregon cabezon	Recruitment	Groundfish	0-200	Eschemeyer et al. 1983; Froese and Pauly 2019
07	WOLINGCD	Washington & Oregon lingcod	Recruitment	Groundfish	0-475	Allen and Smith 1988; Froese and Pauly 2019
08	WOBROCK	Washington & Oregon black rockfish	Recruitment	Groundfish	0-366	Hart 1973; Froese and Pauly 2019
09	WCCANARY	WC canary rockfish	Recruitment	Groundfish	0-838	Love et al. 2002; Froese and Pauly 2019
10	WCDBROCK	WC darkblotched rockfish	Recruitment	Groundfish	25-600	Allen and Smith 1988; Froese and Pauly 2019
11	WCPSOLE	WC petrale sole	Recruitment	Groundfish	0-550	Allen and Smith 1988; Froese and Pauly 2019
12	WCSAB	WC sablefish	Recruitment	Groundfish	175-2740	Allen and Smith 1988; Froese and Pauly 2019
13	WCWIDOW	WC widow rockfish	Recruitment	Groundfish	0-549	Kramer et al. 1995; Froese and Pauly 2019

14	WCHAKE	WC Pacific hake	Recruitment	Small Pelagic	0-1000	Inada 1995; Froese and Pauly 2019
15	WCGROCK	WC greenstriped rockfish	Recruitment	Groundfish	25-425	Allen and Smith 1988; Froese and Pauly 2019
16	WCDSOLE	WC dover sole	Recruitment	Groundfish	0-150	Muus and Nielsen 1999; Froese and Pauly 2019
17	WCESOLE	WC English sole	Recruitment	Groundfish	0-550	Allen and Smith 1988; Froese and Pauly 2019
18	WCATF	WC arrowtooth flounder	Recruitment	Groundfish	18-950	Russian Academy of Science 2000; Froese and Pauly 2019
19	WCCHILI	WC chilipepper rockfish	Recruitment	Groundfish	0-425	Allen and Smith 1988; Froese and Pauly 2019
20	WCBOCACC	WC bocaccio rockfish	Recruitment	Groundfish	0-476	Kramer et al. 1995; Froese and Pauly 2019
21	WCSBROCK	WC shortbelly rockfish	Recruitment	Groundfish	0-350	Allen and Smith 1988; Froese and Pauly 2019
22	WCSNROCK	WC splitnose rockfish	Recruitment	Groundfish	0-800	Allen and Smith 1988; Froese and Pauly 2019
23	WCMACK	WC Pacific mackerel	Recruitment	Small Pelagic	0-400	Riede 2004; Froese and Pauly 2019
24	WCPOP	WC Pacific ocean perch	Recruitment	Groundfish	0-825	Allen and Smith 1988; Froese and Pauly 2019
25	SITHERR	Sitka Sound Pacific herring	Recruitment	Small Pelagic	0-475	Coad and Reist 2004; Froese and Pauly 2019
26	SEYHERR	Seymour Canal Pacific herring	Recruitment	Small Pelagic	0-475	Coad and Reist 2004; Froese and Pauly 2019
27	GOAATF	GOA arrowtooth flounder	Recruitment	Groundfish	18-950	Russian Academy of Science 2000; Froese and Pauly 2019
28	GOADSOLE	GOA dover sole	Recruitment	Groundfish	0-150	Muus and Nielsen 1999; Froese and Pauly 2019
29	GOADKROCK	GOA dusky rockfish	Recruitment	Groundfish	5-160	Orr and Blackburn 2004; Froese and Pauly 2019

30	GOAFSOLE	GOA flathead sole	Recruitment	Groundfish	0-1050	Allen and Smith 1988; Froese and Pauly 2019
31	GOANROCK	GOA northern rockfish	Recruitment	Groundfish	0-740	Russian Academy of Science 2000; Froese and Pauly 2019
32	GOARESOLE	GOA rex sole	Recruitment	Groundfish	0-900	Russian Academy of Science 2000; Froese and Pauly 2019
33	GOARBROCK	GOA rougheye/blackspotted rockfish	Recruitment	Groundfish	170-675	Ou et al. 2016
34	GOAPOLL	GOA walleye pollock	Recruitment	Groundfish	0-1280	Fedorov et al. 2003; Froese and Pauly 2019
35	GOACOD	GOA Pacific cod	Recruitment	Groundfish	10-1280	Fedorov et al. 2003; Froese and Pauly 2019
36	GOAPOP	GOA Pacific Ocean perch	Recruitment	Groundfish	0-825	Allen and Smith 1988; Froese and Pauly 2019
37	KIRCRAB	Kodiak Island red king crab	Recruitment	Invertebrate	20-50	Stevens 2014
38	GOASAB	GOA, EBS & AI Sablefish	Recruitment	Groundfish	175-2740	Allen and Smith 1988; Froese and Pauly 2019
39	NSRCRAB	Norton Sound red king crab	Recruitment	Invertebrate	20-50	Stevens 2014
40	TOHERR	Togiak Pacific herring	Recruitment	Small Pelagic	0-475	Coad and Reist 2004; Froese and Pauly 2019
41	BBRCRAB	Bristol Bay red king crab	Recruitment	Invertebrate	20-50	Stevens 2014
42	SMBCRAB	St. Matthew Island blue king crab	Recruitment	Invertebrate	45-75	Stevens 2014
43	EBSSCRAB	EBS snow crab	Recruitment	Invertebrate	50-80	Stevens 2014
44	EBSPOLL	EBS walleye pollock	Recruitment	Groundfish	0-1280	Fedorov et al. 2003; Froese and Pauly 2019
45	PIRCRAB	Pribilof Islands red king crab	Recruitment	Invertebrate	20-50	Stevens 2014
46	PIBCRAB	Pribilof Islands blue king crab	Recruitment	Invertebrate	45-75	Stevens 2014
47	EBSNROCK	EBS & AI northern rockfish	Recruitment	Groundfish	0-740	Russian Academy of Science 2000; Froese and Pauly 2019
48	EBSNRSOLE	EBS & AI northern rock sole	Recruitment	Groundfish	0-700	Fedorov et al. 2003; Froese and Pauly 2019

49	EBSAKPLC	EBS & AI Alaska plaice	Recruitment	Groundfish	0-600	Fedorov et al. 2003; Froese and Pauly 2019
50	EBSATF	EBS & AI arrowtooth flounder	Recruitment	Groundfish	18-950	Russian Academy of Science 2000; Froese and Pauly 2019
51	EBSRBROCK	EBS & AI rougheye/blackspotted rockfish	Recruitment	Groundfish	170-675	Ou et al. 2016
52	EBSATKA	EBS & AI Atka mackerel	Recruitment	Groundfish	0-720	Kells et al. 2016; Froese and Pauly 2019
53	EBSPOP	EBS & AI Pacific ocean perch	Recruitment	Groundfish	0-825	Allen and Smith 1988; Froese and Pauly 2019
54	AIPOLL	AI walleye pollock	Recruitment	Groundfish	0-1280	Fedorov et al. 2003; Froese and Pauly 2019
55	EBSFSOLE	EBS & AI flathead sole	Recruitment	Groundfish	0-1050	Allen and Smith 1988; Froese and Pauly 2019
56	EBSYFS	EBS & AI yellowfin sole	Recruitment	Groundfish	0-700	Tobor 1972; Froese and Pauly 2019
57	EBSTRBT	EBS & AI greenland turbot	Recruitment	Groundfish	1-2200	Borje and Hareide 1993; Froese and Pauly 2019
58	EBSCOD	EBS & AI Pacific cod	Recruitment	Groundfish	10-1280	Fedorov et al. 2003; Froese and Pauly 2019
59	WKAPOLL	Western Kamchatka walleye pollock	Recruitment	Groundfish	0-1280	Fedorov et al. 2003; Froese and Pauly 2019
60	RUSSCOD	Russian saffron cod	Recruitment	Groundfish	0-300	Fedorov et al. 2003; Froese and Pauly 2019
61	JSDENTEX	Sea of Japan Dentex hypselosomus	Recruitment	Groundfish	50-200	Iwatsuki et al. 2007; Froese and Pauly 2019
62	JSRSBREM	Sea of Japan red seabream	Recruitment	Groundfish	10-200	Nakabo 2002; Froese and Pauly 2019
63	JSPOLL	Sea of Japan walleye pollock	Recruitment	Groundfish	0-1280	Fedorov et al. 2003; Froese and Pauly 2019
64	TSSARD	Tsushima Strait sardine	Recruitment	Small Pelagic	0-200	Whitehead 1985; Froese and Pauly 2019
65	TSRHERR	Tsushima Strait round herring	Recruitment	Small Pelagic	0-40	Fricke et al. 2011; Froese and Pauly 2019

66	TSCMACK	Tsushima Strait chub mackerel	Recruitment	Small Pelagic	0-300	Collette and Nauen 1983; Froese and Pauly 2019
67	TSJMACK	Tsushima Strait jack mackerel	Recruitment	Small Pelagic	0-275	FAO-FIGIS 2005; Froese and Pauly 2019
68	TSAVY	Tsushima Strait anchovy	Recruitment	Small Pelagic	0-400	Fedorov et al. 2003; Froese and Pauly 2019
69	ECSBHAL	East China Sea bastard halibut	Recruitment	Groundfish	10-200	Yamada et al. 1995; Froese and Pauly 2019
70	JFSQUID	Japan winter spawning flying squid	Recruitment	Invertebrate	0-100	FAO-FIGIS 2005
71	JPRSBREM	Japan Pacific coast red seabream	Recruitment	Groundfish	10-200	Nakabo 2002; Froese and Pauly 2019
72	JPCMACK	Japan Pacific coast chub mackerel	Recruitment	Small Pelagic	0-300	Collette and Nauen 1983; Froese and Pauly 2019
73	JPAVY	Japan Pacific coast anchovy	Recruitment	Small Pelagic	0-400	Fedorov et al. 2003; Froese and Pauly 2019
74	JPJMACK	Japan Pacific coast jack mackerel	Recruitment	Small Pelagic	0-275	FAO-FIGIS 2005; Froese and Pauly 2019
75	JPPOLL	Japan Pacific coast walleye pollock	Recruitment	Groundfish	0-1280	Fedorov et al. 2003; Froese and Pauly 2019
76	SBCW_PI	Southern British Columbia & Washington pink salmon	Abundance	Salmon	0-250	Fedorov et al. 2003; Froese and Pauly 2019
77	SBCW_CM	Southern British Columbia & Washington chum salmon	Abundance	Salmon	0-250	Fedorov et al. 2003; Froese and Pauly 2019
78	SBCW_SO	Southern British Columbia & Washington sockeye salmon	Abundance	Salmon	0-250	Fedorov et al. 2003; Froese and Pauly 2019
79	NBC_PI	Northern British Columbia pink salmon	Abundance	Salmon	0-250	Fedorov et al. 2003; Froese and Pauly 2019
80	NBC_CM	Northern British Columbia chum salmon	Abundance	Salmon	0-250	Fedorov et al. 2003; Froese and Pauly 2019
81	NBC_SO	Northern British Columbia sockeye salmon	Abundance	Salmon	0-250	Fedorov et al. 2003; Froese and Pauly 2019
82	SAK_PI	Southeast Alaska pink salmon	Abundance	Salmon	0-250	Fedorov et al. 2003; Froese and Pauly 2019
83	SAK_CM	Southeast Alaska chum salmon	Abundance	Salmon	0-250	Fedorov et al. 2003; Froese and Pauly 2019

84	SAK_SO	Southeast Alaska sockeye salmon	Abundance	Salmon	0-250	Fedorov et al. 2003; Froese and Pauly 2019
85	PW_PI	Prince William Sound pink salmon	Abundance	Salmon	0-250	Fedorov et al. 2003; Froese and Pauly 2019
86	PW_CM	Prince William Sound chum salmon	Abundance	Salmon	0-250	Fedorov et al. 2003; Froese and Pauly 2019
87	PW_SO	Prince William Sound sockeye salmon	Abundance	Salmon	0-250	Fedorov et al. 2003; Froese and Pauly 2019
88	CI_PI	Cook Inlet pink salmon	Abundance	Salmon	0-250	Fedorov et al. 2003; Froese and Pauly 2019
89	CI_CM	Cook Inlet chum salmon	Abundance	Salmon	0-250	Fedorov et al. 2003; Froese and Pauly 2019
90	CI_SO	Cook Inlet sockeye salmon	Abundance	Salmon	0-250	Fedorov et al. 2003; Froese and Pauly 2019
91	KO_PI	Kodiak pink salmon	Abundance	Salmon	0-250	Fedorov et al. 2003; Froese and Pauly 2019
92	KO_CM	Kodiak chum salmon	Abundance	Salmon	0-250	Fedorov et al. 2003; Froese and Pauly 2019
93	KO_SO	Kodiak sockeye salmon	Abundance	Salmon	0-250	Fedorov et al. 2003; Froese and Pauly 2019
94	SAKP_PI	Southern Alaska Peninsula pink salmon	Abundance	Salmon	0-250	Fedorov et al. 2003; Froese and Pauly 2019
95	SAKP_CM	Southern Alaska Peninsula chum salmon	Abundance	Salmon	0-250	Fedorov et al. 2003; Froese and Pauly 2019
96	SAKP_SO	Southern Alaska Peninsula sockeye salmon	Abundance	Salmon	0-250	Fedorov et al. 2003; Froese and Pauly 2019
97	WAK_CM	Western Alaska chum salmon	Abundance	Salmon	0-250	Fedorov et al. 2003; Froese and Pauly 2019
98	WAK_PI	Western Alaska pink salmon	Abundance	Salmon	0-250	Fedorov et al. 2003; Froese and Pauly 2019
99	WAK_SO	Western Alaska sockeye salmon	Abundance	Salmon	0-250	Fedorov et al. 2003; Froese and Pauly 2019
100	EKA_PI	Eastern Kamchatka pink salmon	Abundance	Salmon	0-250	Fedorov et al. 2003; Froese and Pauly 2019
101	EKA_SO	Eastern Kamchatka sockeye salmon	Abundance	Salmon	0-250	Fedorov et al. 2003; Froese and Pauly 2019

102	EKA_CM	Eastern Kamchatka chum salmon	Abundance	Salmon	0-250	Fedorov et al. 2003; Froese and Pauly 2019
103	WKA_PI	Western Kamchatka pink salmon	Abundance	Salmon	0-250	Fedorov et al. 2003; Froese and Pauly 2019
104	WKA_CM	Western Kamchatka chum salmon	Abundance	Salmon	0-250	Fedorov et al. 2003; Froese and Pauly 2019
105	WKA_SO	Western Kamchatka sockeye salmon	Abundance	Salmon	0-250	Fedorov et al. 2003; Froese and Pauly 2019
106	RUS_PI	Russia pink salmon	Abundance	Salmon	0-250	Fedorov et al. 2003; Froese and Pauly 2019
107	RUS_CM	Russia chum salmon	Abundance	Salmon	0-250	Fedorov et al. 2003; Froese and Pauly 2019
108	RUS_SO	Russia sockeye salmon	Abundance	Salmon	0-250	Fedorov et al. 2003; Froese and Pauly 2019
109	J_PI	Japan pink salmon	Abundance	Salmon	0-250	Fedorov et al. 2003; Froese and Pauly 2019
110	CCZOOW	CC zooplankton winter	Biomass	Zooplankton	0-400	Goericke et al. 2014
111	CCZOOSP	CC zooplankton spring	Biomass	Zooplankton	0-400	Goericke et al. 2014
112	CCZOOSU	CC zooplankton summer	Biomass	Zooplankton	0-400	Goericke et al. 2014
113	CCZOOF	CC zooplankton fall	Biomass	Zooplankton	0-400	Goericke et al. 2014
114	EBSBZOO	EBS basin zooplankton	Biomass	Zooplankton	200-2000	Eisner et al. 2014
115	EBSOSZOO	EBS outer shelf zooplankton	Biomass	Zooplankton	100-200	Eisner et al. 2014
116	EBSMSZOO	EBS mid shelf zooplankton	Biomass	Zooplankton	50-100	Eisner et al. 2014
117	EBSCZOO	EBS coastal zooplankton	Biomass	Zooplankton	0-50	Eisner et al. 2014
118	JOZOOSP	Oyashio Current zooplankton spring	Biomass	Zooplankton	0-2000	Ikeda et al. 2008
119	JOZOOSU	Oyashio Current zooplankton summer	Biomass	Zooplankton	0-2000	Ikeda et al. 2008
120	BSJELLY	EBS large medusae jellyfish	Relative CPUE	Zooplankton	10-40	Brodeur et al. 2002

Table 2.2. Eight climate indices.

Abbreviation	Name	Description	Data source	Reference
Global SSTA	Global-ocean averaged SST anomaly	SST anomalies are averaged over the global ocean	Calculated from COBE SST version 2	None
NP SSTA	NP averaged SST anomaly	SST anomalies are averaged over the NP, north of 20°-68°N		
PDO	Pacific Decadal Oscillation	Dominant pattern of North Pacific SST variability north of 20°N (annual)	University of Washington, Joint Institute for the Study of the Atmosphere and Ocean	Mantua et al. 1997
NPGO	North Pacific Gyre Oscillation	Second dominant pattern of sea surface height variability in the Northeast Pacific (annual)	Emanuele Di Lorenzo, Georgia Institute of Technology	Di Lorenzo et al. 2008
MEI	Multivariate El Nino-Southern Oscillation	Dominant pattern of variability of six observed variables over the tropical Pacific (annual)	NOAA Earth System Research Laboratory	Wolter and Timlin 2011
ALPI	Aleutian Low-Pressure Index	Index of the relative intensity of the Aleutian Low-pressure system Dec-Mar (annual)	Fisheries and Oceans Canada	Beamish et al. 1997
NPI	North Pacific Index	The area-weighted sea level pressure over the region 30°N-65°N, 160°E-140°W (annual)	NOAA Earth System Research Laboratory	Trenberth and Hurrell 1994
AO	Arctic Oscillation Index	Dominant pattern of sea level pressure variability north of 20°N (annual)	NOAA Climate Prediction Center	Thompson and Wallace 1998

Table 2.3. Correlations between marine ecosystem PCs and climate indices. Asterisks indicate significant correlations at the 95% confidence level.

	Global SSTA	NP SSTA	PDO	NPGO	MEI	ALPI	NPI	AO
Whole NP EOF1	**0.76***	**0.71***	-0.14	0.03	0.16	0.07	-0.1	0.21
Eastern NP EOF1	**0.75***	**0.57***	0.08	-0.04	0.28	0.21	-0.23	0.25
Western NP EOF1	**0.69***	**0.76***	-0.24	0.08	0.08	-0.07	0.02	0.22
Eastern NP EOF2	0.03	-0.15	**0.56***	-0.09	**0.40***	0.16	-0.2	0.21
Western NP EOF2	0.38	0.15	-0.03	**0.39***	-0.01	0.24	-0.11	-0.04

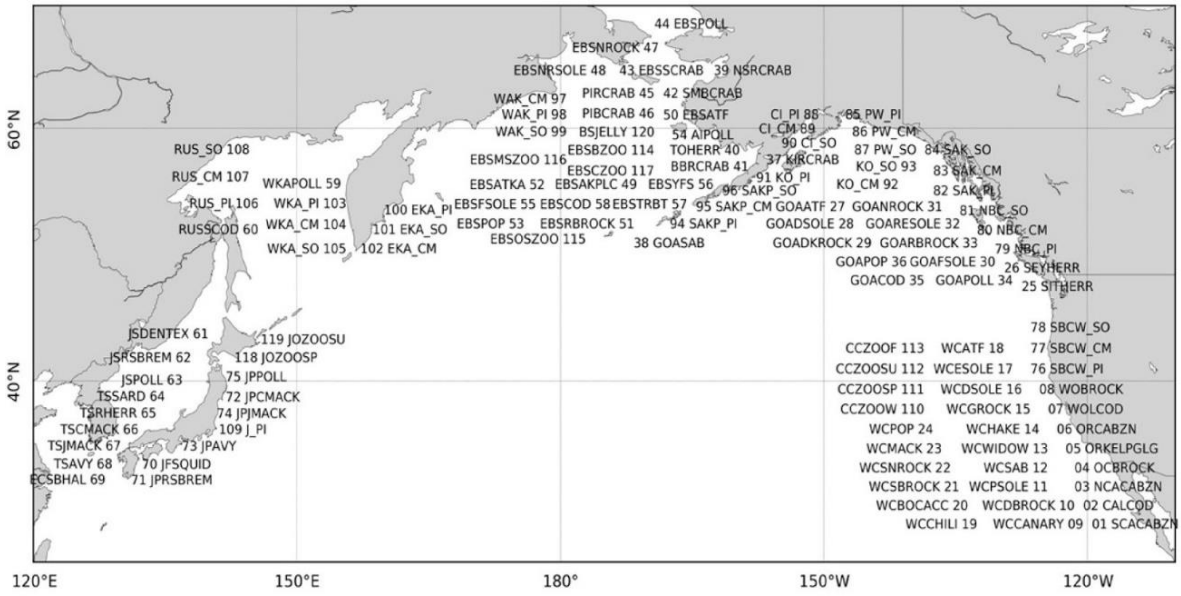

Figure 2.1. Abbreviations for the 120 marine species data from the western NP (the Sea of Japan and the Okhotsk Sea) and eastern NP (the west coast of the United States, Gulf of Alaska and the Bering Sea). See Table 2.1 for a definition of each abbreviations.

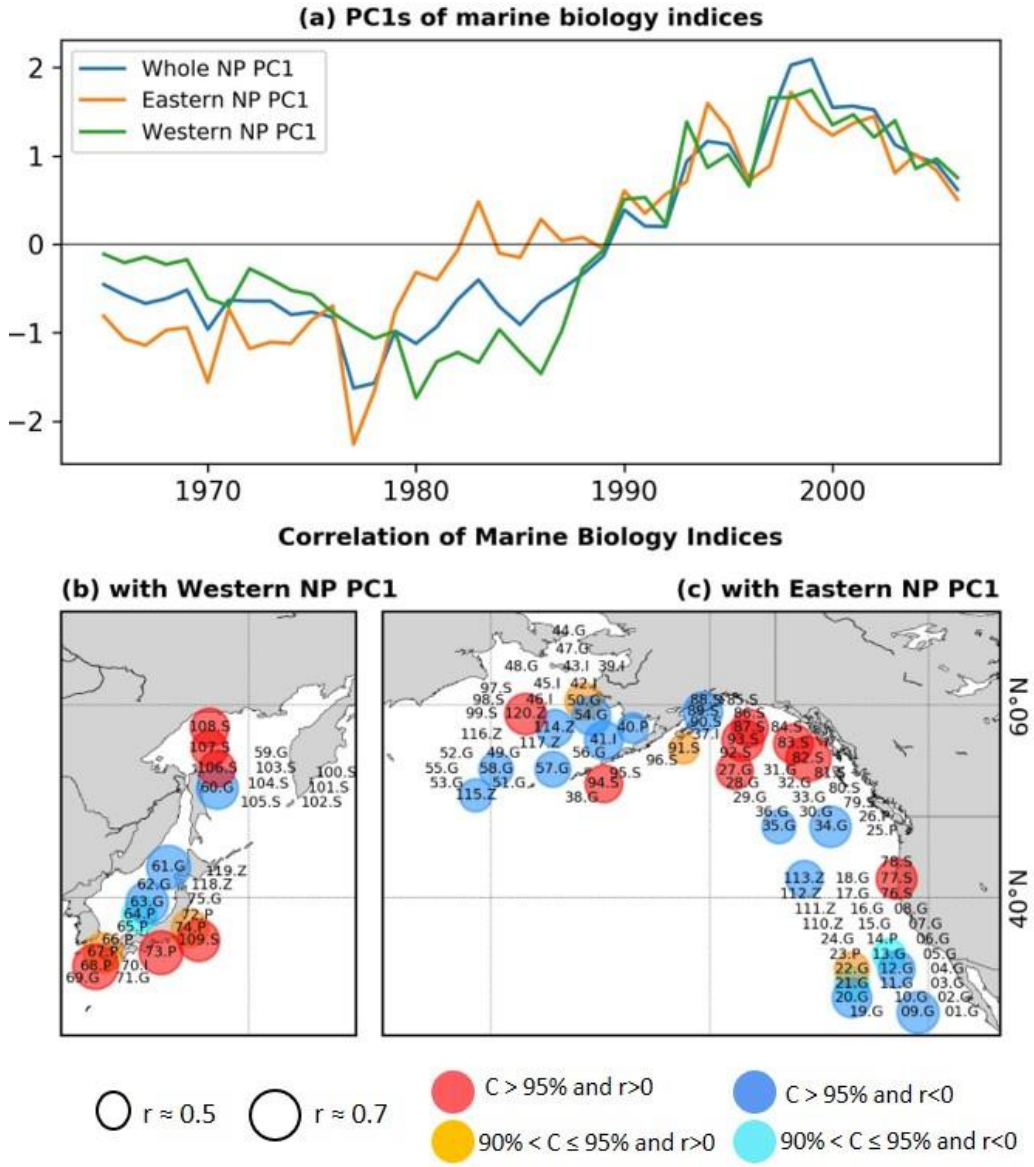

Figure 2.2. (a) PC1s for the whole NP EOF1, eastern NP EOF1 and western NP EOF1 of marine biological, and statistically significant correlations of marine biological indices (b) with the western NP PC1 and (c) with the eastern NP PC1. In (b) and (c), numbers indicate species IDs shown in Table 2.1, while S, G, P, Z and I indicate salmon, groundfish, small-pelagic fish, zooplankton and invertebrates, respectively. Circle size indicates the absolute values of correlations and colors of the circles (red, orange, cyan, blue) indicate the sign of correlations and the corresponding confidence levels

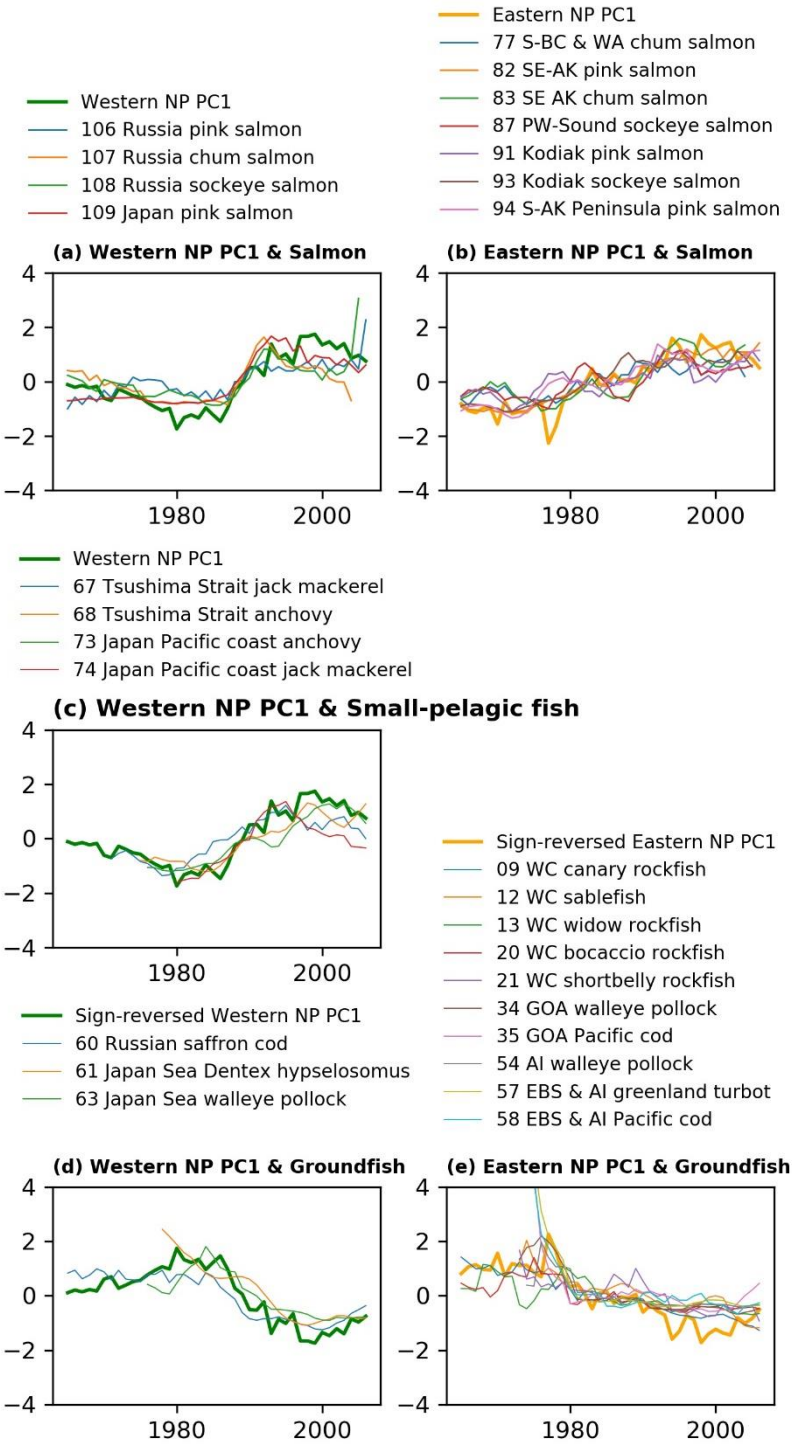

Figure 2.3. Time-series comparison between marine biology PC1 and biological time series that have significant correlation with that PC1 in each basin. Left and right panels show results for the western and eastern basins, respectively, and top, middle, and bottom panels show results for salmon, small-pelagic fish, and groundfish. All-time series smoothed by 5-year running average. For easier comparison, the PC2 time sereis are sign-reversed (multiply by -1) for (d) and (e).

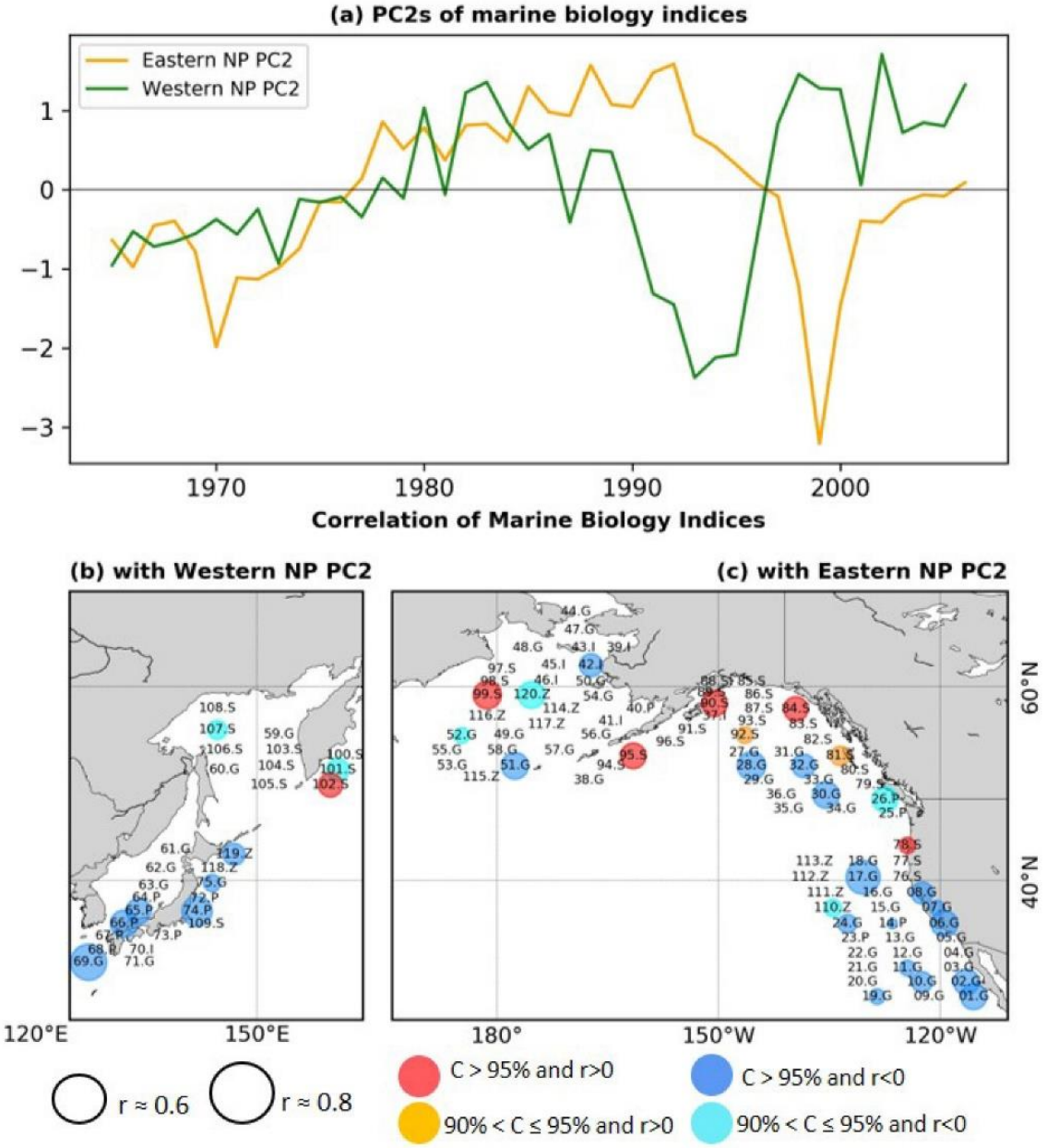

Figure 2.4. Same as in Figure 2.2, but for the EOF 2.

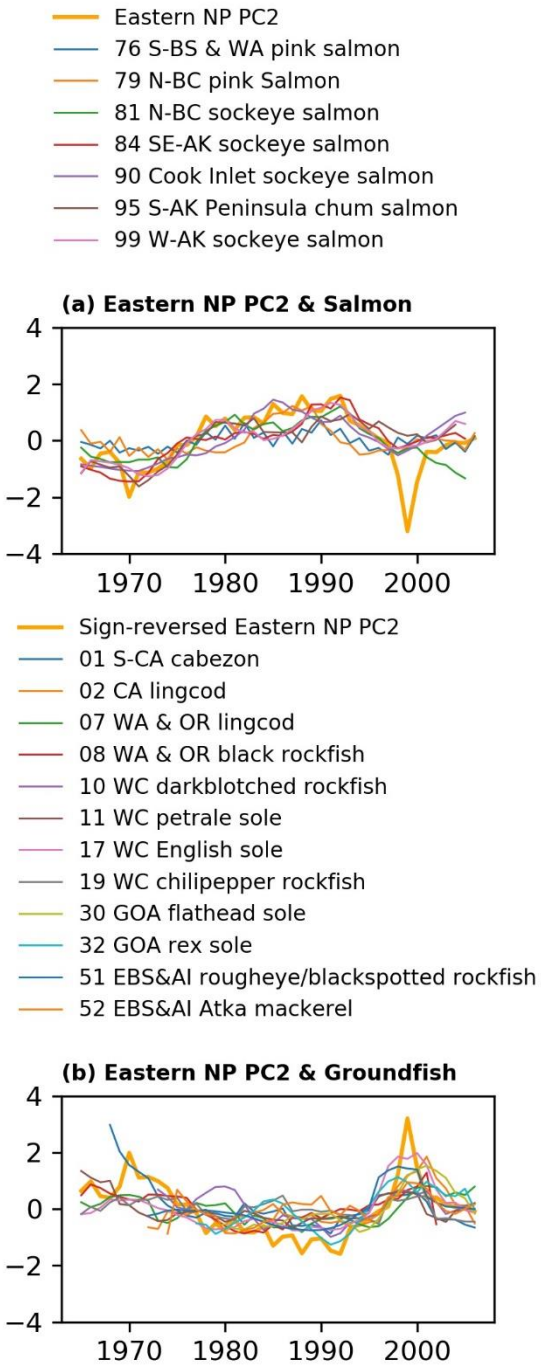

Figure 2.5. Same as in Figure 2.3, but for eastern NP PC2 along with (a) salmon and (b) groundfish.

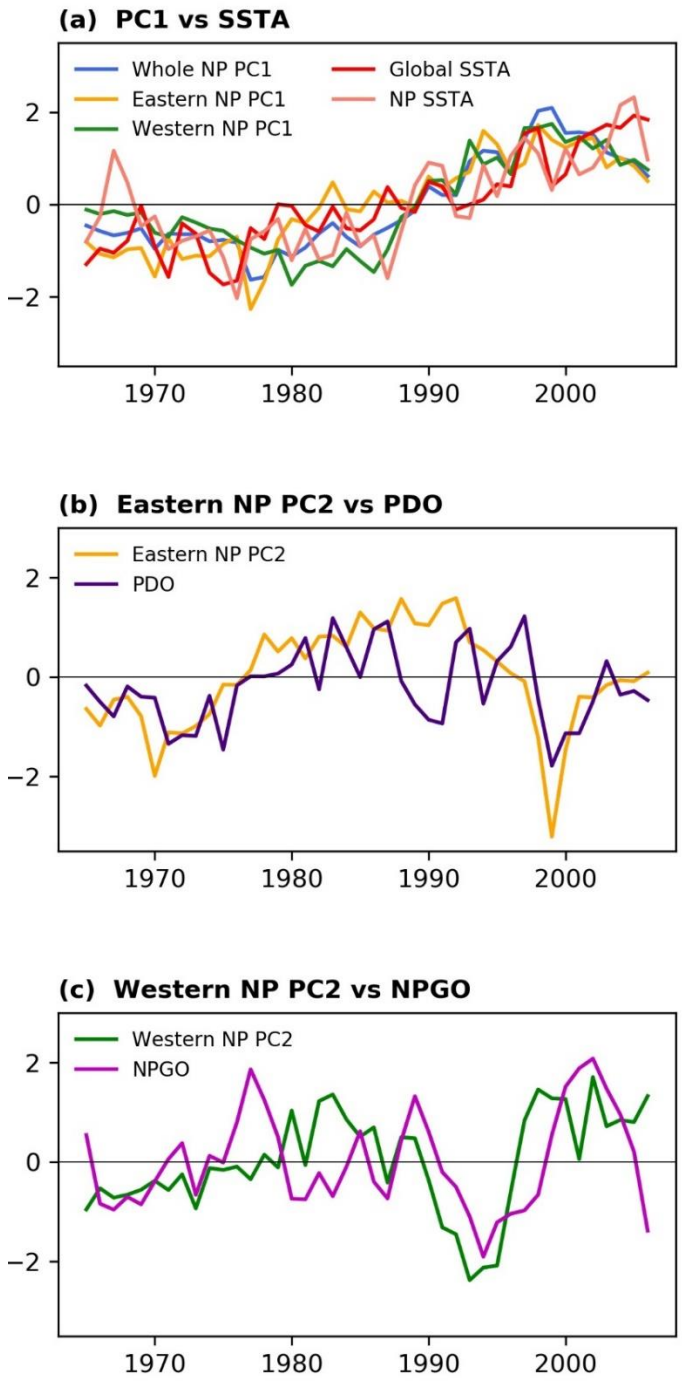

Figure 2.6. (a) PC1s of marine ecosystem and global and NP averaged SSTs, (b) eastern NP PC2 and PDO, and (c) western NP PC2 and NPGO.

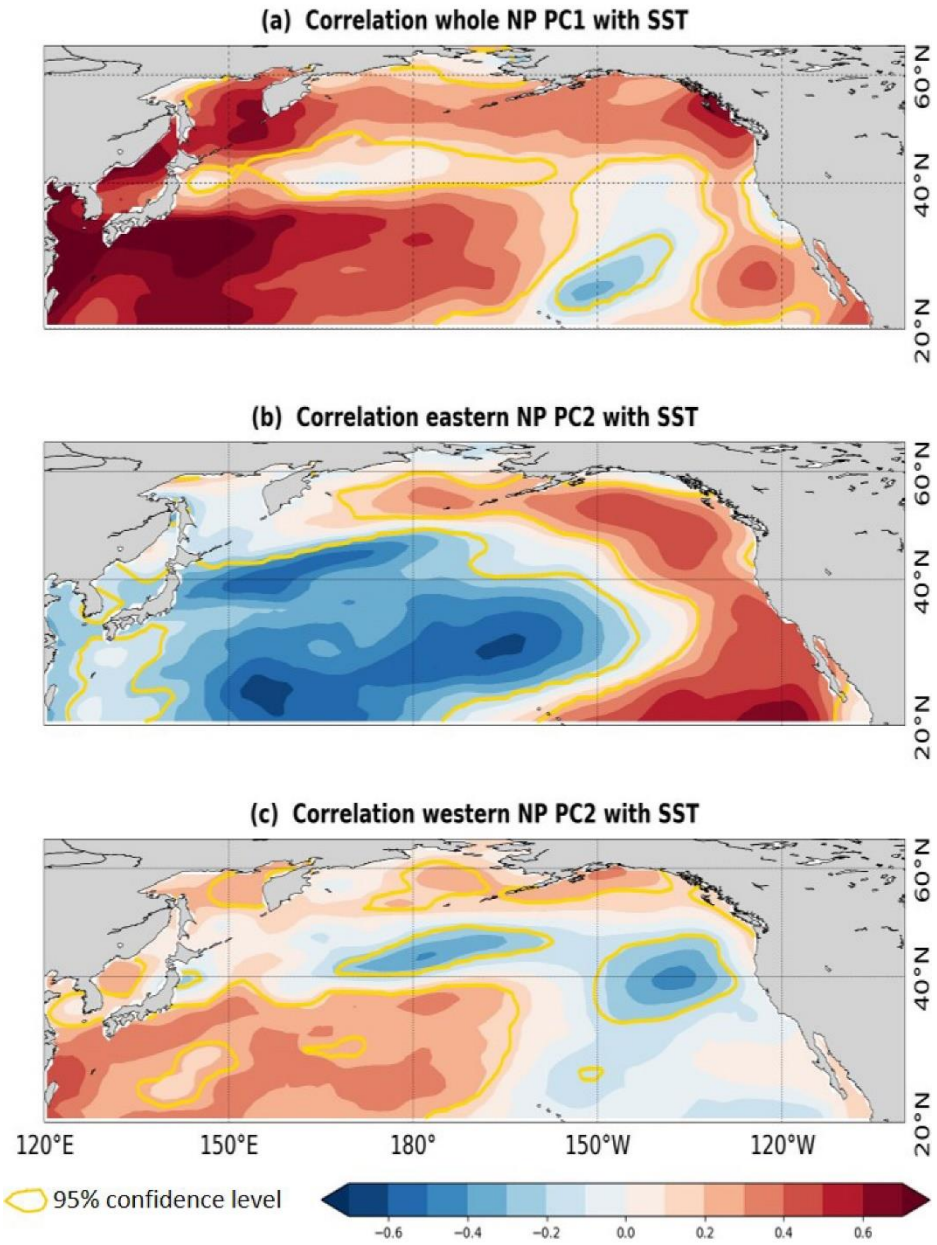

Figure 2.7. Correlation between SST and (a) whole NP PC1, (b) eastern NP PC2, and (c) western NP PC2. The color corresponds with the correlation coefficient and yellow contours indicate the area where correlations are significant at the 95% confidence level.

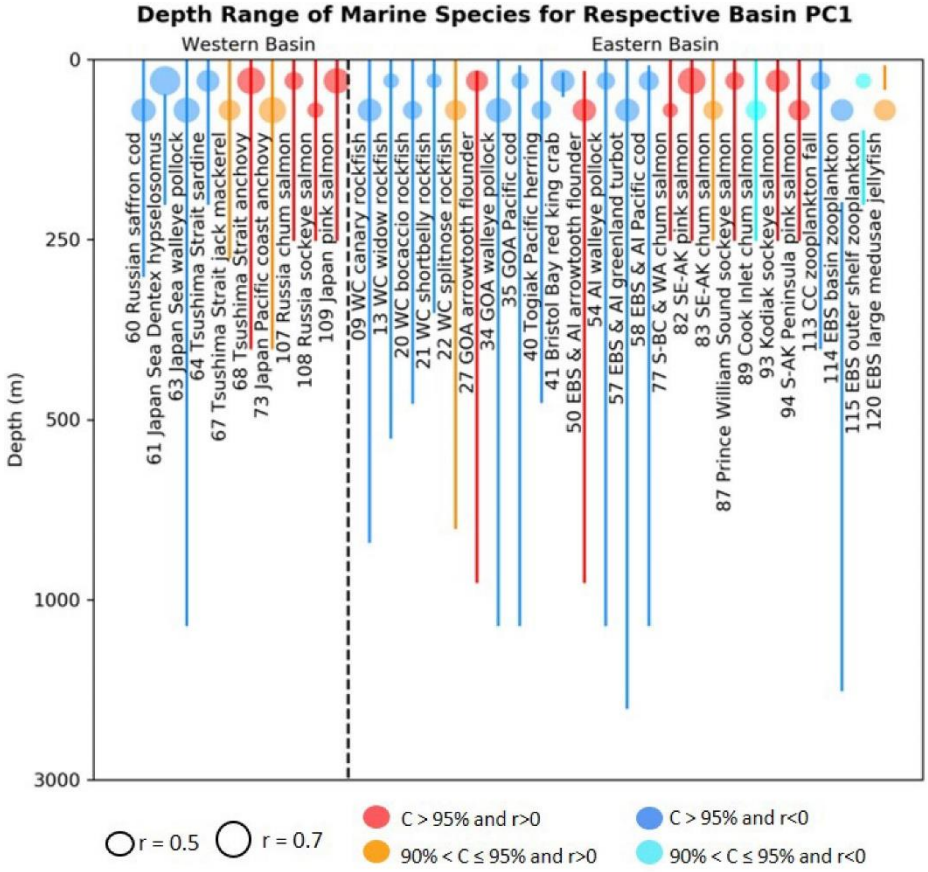

Figure 2.8. Depth ranges (lines) of western and eastern basin marine biology data that have statistically significant correlated (colored circles) with respective basin PC1s. Circles indicate the absolute correlations and colors indicate the corresponding confidence levels, as in Figure 2.2.

Chapter 3

Sea Surface Temperature Predictability in the North Pacific From the Latest Seasonal Forecast Systems of the ECMWF, CMCC, and DWD

3.1. Introduction

Seasonal forecasts over the North Pacific (NP) remain challenging, because generally low-predictability in mid and high latitudes compared with higher predictability in the tropics, where air-sea coupled phenomena, such as the El Niño Southern Oscillation (ENSO), provide a long memory (e.g., Doi et al. 2016; Johnson et al. 2019). Prediction skill for sea surface temperatures (SST) and 2-m air temperatures over the NP have common spatial structures across different studies (e.g., Becker et al. 2014; Doi et al. 2016; Johnson et al. 2019). In the winter, prediction skills are generally high in the eastern NP, especially in the Gulf of Alaska (GOA) and in the central NP north of Hawaii, but are generally low in the region between the Kuroshio Extension and the subpolar front to the east of Japan. Overall prediction skills patterns in the summer follow a similar pattern to that in winter; however, prediction skills in the summer are low in the north of Hawaii.

The predictability of seasonal forecast system can be related to inertia (memory) and patterns of variability. The SST and upper ocean heat content in anomalies conditions can take relatively long (days to years) decay and can have significant impact

on the atmosphere above. This coupled ocean-atmosphere interaction in the climate system arises interannual climate variability, such as ENSO. ENSO is a prominent couple mode involving the tropical Pacific which induce climate anomalies around the globe via teleconnection (Alexander et al. 2002). Consequently, a realistic ENSO pattern is an important aspect for the successful seasonal forecasting system (e.g., Johnson et al. 2019). The representation of ENSO on the seasonal SST prediction skill are of focus in this study.

Prediction skill for the SST can be evaluated by correlations at each grid point between an ensemble mean and observed SST. The ensemble mean is formed by averaging ensemble members of a forecast system. The ensemble mean represents the predictable component, whereas the ensemble spread (or ensemble members standard deviation) represent the stochastic component (or the uncertainty of the predictions). The small ensemble spread means that each ensemble member of the forecast system is equally likely to occur, while the large ensemble spread means high uncertainty of the forecast system (Kirtman et al. 2014). Given that, the predictability can be associated with the size of ensemble spread and close co-variability between the ensemble mean and observation. Therefore, it is interesting to know how ensemble members and observations are related, associated with the prediction skills and the large ensembles members are needed to clarify these relations,.

Large ensemble members have recently been applied to seasonal forecasting systems. Doi et al. (2019) conducted 108 ensemble seasonal forecast experiment using a single model, but multi-model ensembles are more frequently used to obtain large ensemble members. The one of multi-model large ensemble projects for the seasonal forecast is organized as North American Multimodel Ensemble (NMME) (Kirtman et

al. 2014) and by using 109 ensembles from nine modelling centers in NMME, Becker et al. (2014) reported the predictability of global SST. Moreover, Copernicus Climate Change Services (C3S) in Europe also provide the operational multi-model seasonal forecasting system since October 2019, involving five centers in Europe and one in the United States. This forecasting system is the successor of the earlier EUROSIP project provided by European Centre for Medium-Range Weather Forecasts (ECMWF). The multi model seasonal forecasting systems which provide by those climate center make it possible to analyze SST predictability in the NP including the relationships among ensemble members and observations based on large ensemble members. The seasonal forecast of C3S is global; however, publications using these datasets focused their attention on Europe sector (e.g., Samaniego et al. 2019; Wander et al. 2019) to the author's knowledge.

Therefore, the purpose of this study was to investigate the SST predictability over the North Pacific including the relations between ensemble members and observation, by analyzing seasonal forecasting datasets of C3S. Three models in C3S were used in this study (i.e., the latest seasonal forecast systems of ECMWF, Deutscher Wtterdienst (DWD) and Centro-Euro-Mediterraneo Sui Cambiamenti Climatici (CMCC)), because these forecasting systems were initialized each year on the 1st day of the starting month, unlike other models in C3S.

3.2. Data and Methods

Monthly SST hindcasts (reforecast) in 1994-2016 (23 years) for January and July forecast with a lead time of 3 months from seasonal forecast ECMWF system 5,

DWD system 2, and CMCC system 3 were used for forecast data. For January (July) forecast with the 3-month lead time, the initialization date was November (May) 1st. The seasonal forecast from ECMWF system 5, DWD system 2, and CMCC system 3 are coupled atmosphere-ocean model. Hereinafter, the names of the modeling centers are used to distinguish the models for simplicity. The forecast system specification along with the ensemble size of each model can be seen in Table 3.1.

The multi model ensemble member was obtained by combining the ensemble members produce by ECMWF, DWD and CMCC. Thus, the total ensemble size of multi model ensemble, used in this study, was 95 ensemble members. Moreover, SST ensemble mean of respective model is formed by averaging the ensemble members of each model, while SST of multi-model ensemble mean (MMEM) is formed by averaging together the ensemble member of three models (ECMW, DWD and CMCC).

Monthly SST data of Centennial in Situ Observation-Based Estimates of the Variability of SST and Marine Meteorological Variables (COBE SST) version 2 reanalysis data (Hirahara et al. 2014) in 1994-2016 for the January and the July were used as observed SST for model verification.

The temporal correlation anomalies between Multi Model Ensemble Mean (MMEM) and observed SST anomalies (SSTs) were examined. The temporal correlation between MMEM and observed SSTs is a widely used as estimator of the prediction skill (e.g., Becker et al. 2014; Jacox et al. 2019). This correlation can be calculated for two time series either at each grid point (referred to the point-wise correlation) or for the area-averaged time series. Therefore, this study also used three region of interest i.e., the Kuroshio-Oyashio Extensions (35˚-41˚N, 145˚-150˚E), the

Central NP (31˚-36˚N, 160˚-170˚E), and the Gulf of Alaska in the eastern NP (53˚-57˚N, 140˚-150˚W) to analysis the relation of ensemble members and observation.

The distribution of temporal correlation between MMEM, ensemble members and observed SSTs at area averaged of those regions interest were plotted in histogram. Two criteria were used to assess the relation ensemble members and observation in the histogram. First, if the correlation between the MMEM and observation is located within the range of correlations distribution of MMEM with the respective ensemble members, the forecast system reasonably captures observation as an ensemble member. Second, if the correlation between the MMEM and observation is not within the range of the distribution (or as outlier) of correlations between MMEM and respective ensemble members, the forecast system fails to capture observation and shows biased variability. An outlier is a value that lies out of correlation distribution between MMEM and ensemble members.

Furthermore, the correlation map between area-averaged time series (i.e., Kuroshio Oyahio Extension (KOE), Central North Pacific and Gulf of Alaska (GOA)) and SSTs at grid points over the North and tropical Pacific Ocean for MMEM and observation in January and July were also analyzed, to understand the relation of SST predictability in NP with the Niño region.

Statistical significance was evaluated by using a Monte-Carlo Simulation. In Monte-Carlo Simulation, some steps were performed to evaluate the significance of the relationship between MMEM and observed SST. First, by using red noise model, 100 surrogate time series for the MMEM with lag-1 correlation estimated by using Burg's method were generated. Then, surrogate correlation coefficients were calculated for

each grid point between observed SST and the surrogate MMEM. The percentile of the absolute value of the observed correlation with the absolute values of surrogate correlations gives the confidence level.

3.3. Results

Figure 3.1 shows the prediction skill expressed by the point-wise correlation between MMEM and observed SSTs for the January forecast. Prediction skills was low in the western NP around Japan, especially between the Kuroshio Extension and the subpolar front to the east of Japan, which is often called the Kuroshio-Oyashio Extensions (KOE), and around the subpolar front in the Sea of Japan. In contrast, high skills occur in the central and eastern NP.

Figure 3.2 shows histogram of temporal correlations for area-averaged SSTs between MMEM and ensemble members along with the correlation between MMEM and observed SSTs for the January forecast in each of three areas. For the KOE, correlation between MMEM and observed SSTs was the lower than 2.1 percentile of the correlations between MMEM and ensemble members, indicating that the observed variability is an outlier. This indicates that the low prediction skill of MMEM over the KOE is associated with the biased prediction which does not capture the observation within the range of the distribution of ensemble members. For the Central NP and the GOA, the correlation between MMEM and observation was high and was in the middle of the correlations between MMEM and ensemble members, which are more narrowly clustered than those for the KOE. This suggests that high prediction skill in these regions are associated with the strong predictable component relative to unpredictable

stochastic component and with reasonable distribution of ensemble members so that the observation can be regarded as an ensemble member.

Figure 3.3 shows time series of the area averaged time series for MMEM, ensemble members and observed SST anomalies to analyzed the spread of ensemble members and the temporal variability of ensemble members, ensemble mean and observation at area averaged of the KOE, central NP and GOA. For the central NP and the GOA, ensemble members show common variability around the MMEM, and the observed variation is close to the MMEM. For the KOE, on the other hand, ensemble members and MMEM still show common variability, but observation show different variability. These results are consistent with the major features in Figure 3.2.

Low prediction skill areas were more widely distributed in July than in January (Figure 3.4). Prediction skills in July were high along the California water, the GOA and the Bering Sea and. On the other hand, prediction skills were low around the Sea of Japan, the Okhotsk Sea, some area of central NP and the East China Sea.

Histogram of temporal correlations for area-averaged SSTs of the regions of interest shows three different relations between ensemble member and observation (Figure 3.5). For the GOA, the high temporal correlation between MMEM and observation was in the range of distribution of the temporal correlations between MMEM and ensemble members and was not an outlier corresponding to the top 5%. Although low prediction skill occurs in both the KOE and the central NP areas, the relations between ensemble members and observation are different between two regions. For the central NP, the correlation between MMEM and observation becomes an outlier for correlations between MMEM and ensemble members, as found for the

KOE in January. For the KOE in July, on the other hand, the correlation between MMEM and observation is in the middle of a widely distributing correlations between MMEM and ensemble members. This suggests that for the July KOE the observation can be regarded as an ensemble, but the wide ensemble spread causes the low prediction skill.

Consistent with the histogram analysis, time series of respective regions for July forecast show different features in different areas (Figure 3.6). For the GOA, common variations were occurred in MMEM, ensemble members and observation. For the central NP, common variation in MMEM and ensemble members was not shared by the observations. For the KOE, some common variations across ensemble members was found around 2000-2010 but MMEM and observation were exhibits unrelated variability.

Consequently, low predictability is associated with two different types of relations between ensemble members and observations. One is successful capture of observational feature by ensemble members but with wide ensemble spread. The other is the unsuccessful capture of observational features by ensemble members. The former case explains the low predictability in the July KOE, while the latter applies to the July central NP and the January KOE.

Figure 3.7 and 3.8 show the MMEM and the observed SSTs correlation map between area averaged SSTs of regions of interest (the KOE, the central NP and the GOA) and SSTs at grid points from the North to tropical Pacific Ocean, in January and July. As expected, the strong significant positive correlation in the vicinity of the areas

of interest (i.e., black outlines mark the regions of interest in Figure 3.7 and 3.8) can be seen in the MMEM correlation map and the observation correlation map.

Observed SST in NP basin and ENSO in the tropical Pacific were likely a source of low SST predictability in KOE and the central NP. MMEM SSTs correlation map of KOE in January show significant correlation in Niño region and mostly no significant correlation in NP basin, while observed SSTs correlation map of KOE does not show significant correlation in Niño region (Figure 3.7(a,d)). MMEM and observed SSTs correlation map of the central NP in July doesn't show significant correlation in Niño region but show different significant correlation patterns in NP basin SSTs (Figure 3.8(b,e)). The result in the January KOE and the July central NP correlation maps between MMEM and observation (Figure 3.7(a,d) and 3.8(b,e)) were consistent with low SST predictability due to model cannot capture observation (Figure 3.2(a) and 3.5(b)). On the other hand, MMEM and observed SSTs of KOE in July doesn't show significant correlation in Niño region and show mostly no significant correlation in NP basin (Figure 3.8(a,d)). The correlation maps in the July KOE between MMEM and observation show similar low correlation spatial pattern in NP basin and Niño region, which consistent with low SST predictability due to low correlation between MMEM and observation (Figure 3.5(a)).

The high SST predictability in the central NP in January were associated with observed SST in NP basin and ENSO in the tropical Pacific. MMEM and observed SSTs correlation map of the central NP in January show significant correlation in Niño region and significant correlation were mostly found in NP basin (Figure 3.7(b,e)). These results consistent with the histogram analysis which found that SST predictability in the central NP in January was high due model can capture observation (Figure 3.2(b)).

However, observed SST in NP basin and ENSO in the tropical Pacific are likely a source of high SST predictability in GOA only in July. It is because MMEM and observed SSTs correlation map of the GOA in July show significant correlation in Niño region and significant correlation from NP basin to tropical Pacific (Figure 3.8(c,f)). On the other hand, MMEM SSTs correlation map of the GOA in January show significant correlation in the Niño region and around NP basin to tropical Pacific (Figure 3.7 (c)), while observed SSTs correlation map of the GOA only show significant correlation around the Bering Sea, the GOA and the California water (Figure 3.7 (f)). This indicate that only observed SSTs in NP basin is likely source of SST predictability in GOA in January.

Next, the ensemble members of respective models were analyzed. Figures 3.9 (a)-(c) and 3.10 (a)-(c) show the predictions skill of respective model ensemble mean (RMEM) for January and July forecast, respectively. The patterns of prediction skill of RMEM were similar with those for MMEM shown in Figures. 3.1 and 3.4. These results indicate that the regionality and seasonality of prediction are robustly determined by common mechanism operating across models. It is interesting to note that high prediction skill in the downstream the KOE was detected in all three models. Figures 3.9 (d)-(f) and 3.10 (d)-(f) show the difference in prediction skill, that is defined as the MMEM prediction skill minus RMEM prediction skill. As expected, the difference is generally positive; that is, MMEM prediction skills are generally higher than RMEM prediction skills. The magnitudes of difference are similar for the ECMWF and CMCC forecast systems and were large for the DWD system compared with the other two models. The relatively coarse model resolution of the DWD forecast system compared with the other two models (Table 3.1) might explain the large prediction skill difference.

3.4 Summary and Discussion

The SST predictability in MMEM over the NP was analyzed by using the latest seasonal forecast system of ECMWF, DWD and CMCC from C3S for the winter (January) and summer (July), with a focus on three regions of interest, i.e. the KOE, the central NP and the GOA. The high correlation between MMEM and observed SSTs in the GOA and central NP in January and in the GOA in July reflects the fact that the model successfully capture the interannual variability of observed SSTs accompanied by a small ensemble spread (Figure 3.1, 3.2(b,c), 3.3(b,c), 3.4, 3.5(c), 3.6(c)). A low prediction skill due to a small spread among ensemble members, but ensemble model cannot to capture the observation, are found in the January KOE and in the July central NP (Figure 3.1, 3.2(a), 3.3(a), 3.4, 3.5(b), 3.6(b)). On the other hand, A low prediction skill due to a large ensemble spread is found in the KOE for July forecast (Figure 3.4, 3.5(a), 3.6(a)). A small ensemble spread but ensemble members cannot capture the observation is resulted from common biased variations among ensemble members.

The high SST predictability in the central NP in January and the GOA in both the January and July and were consistent with previous studies (Becker et al. 2014; Doi et al. 2016; Johnson et al. 2019). Observed SSTs in NP basin and ENSO variability were likely a source for high SST predictability in the central NP in January. The relation of ENSO in the tropical Pacific also can be seen from the significant correlation in Niño region, as seen in MMEM and observed SSTs correlation map in the central NP in January (Figure 3.7(b,e)). As known, ENSO in the tropical Pacific can influence SST variation in the North Pacific via atmospheric bridge (Alexander et al. 2002). The ENSO-driven large-scale atmospheric teleconnection alters the near-surface air

temperature, humidity, wind and the distribution of clouds from the equatorial Pacific to the North Pacific and affects SST variability in the North Pacific. However, observed SST in NP basin and ENSO in the tropical Pacific were likely a source of high SST predictability in the GOA only in July (Figure 3.8(c,f)), because high SST predictability in the GOA in January was likely due to observed SST in NP basin (Figure 3.7(c,f)). The significance correlation in Niño region did not found in the observed SSTs correlation map for the GOA in January (Figure 3.7(f)).

The low prediction skill in the KOE both in January and July in central NP in July were also consistent to previous studies (Becker et al. 2014; Doi et al. 2016; Johnson et al. 2019), but in those studies the relation among ensemble members and observation were not examined. Further analysis also reveals that observed SSTs in NP basin and ENSO variability were also likely a source for low SST predictability in the KOE and the central NP. The MMEM and observed SSTs show that low SST predictability due to model cannot capture observation, as seen in the KOE in January (Figure 3.7(a,d) and the central NP in July (Figure 3.8(b,e)), or because overall correlation in NP basin and Niño region were low as seen in MMEM and observed SSTs correlation map for the KOE in July (Figure 3.8(a,d). It is also generally considered that the variations in the KOE are difficult to be predicted due to chaotic oceanic variability caused by strong currents. The chaotic variability will cause a large ensemble spread, but the analysis in this study indicates that not only the ensemble spread is the source of the low predictability, but also biased variations across ensemble members are important, as found in the KOE in January and the central NP in July.

The prediction skill difference, that is defined as the MMEM prediction skill minus RMEM prediction skill, is generally positive. This indicate that MMEM

prediction skills are generally higher than RMEM prediction skills, as expected (Figures 3.9 (d)-(f) and 3.10 (d)-(f)), primarily because MMEM have larger number of ensembles (Becker et al. 2014; Kirtman et al. 2014). The similar patterns between prediction skill of RMEM and MMEM indicate that the regionality and seasonality of prediction are robustly determined by mechanisms which commonly occur across models.

Table 3.1 Hindcast specification from ECMWF, DWD, and CMCC.

Center	System	Ensemble size	Atmos Horizontal resolution /Vertical levels	Ocean Horizontal resolution /Vertical levels
ECMWF	SEAS5 (System 5)	25 members	TCO319 (~36km)/L91	0.25°/L75
DWD	GCFS 2.0 (System 2)	30 members	T127 (~100km)/ L95	(0.4°) on a tripolar grid/L40
CMCC	SPSv3 (System 3)	40 members	1°/L46	0.25°/L50

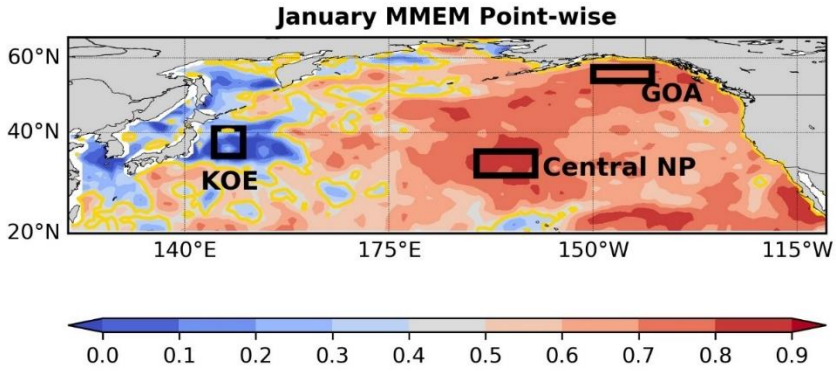

Figure 3.1. Point-wise correlation between MMEM and observed SSTs for the January forecast. Black rectangles indicate regions of interest, i.e., the KOE, the central NP, and the GOA. Colors indicate point-wise correlation between MMEM and observed SSTs, and the yellow contour indicates the area where correlations are significant at the 95% confidence level.

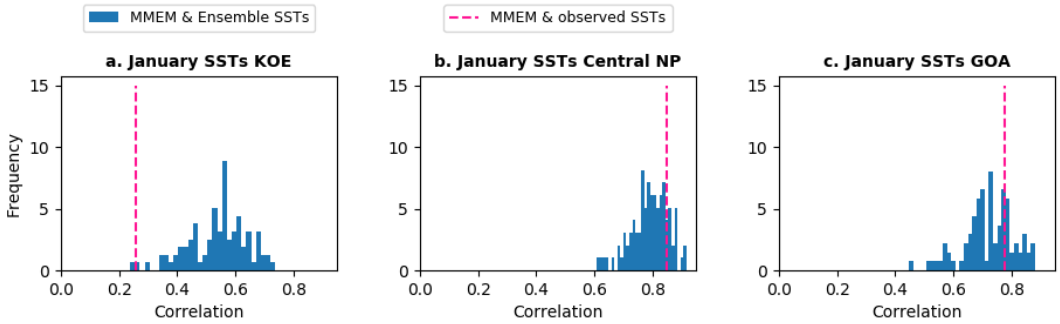

Figure 3.2. Histogram of correlation between MMEM and ensemble members (blue color bars) and correlation between MMEM and observation (vertical pink dashed line) at area averaged for the January forecast over (a) the KOE, (b) the Central NP, and (c) the GOA.

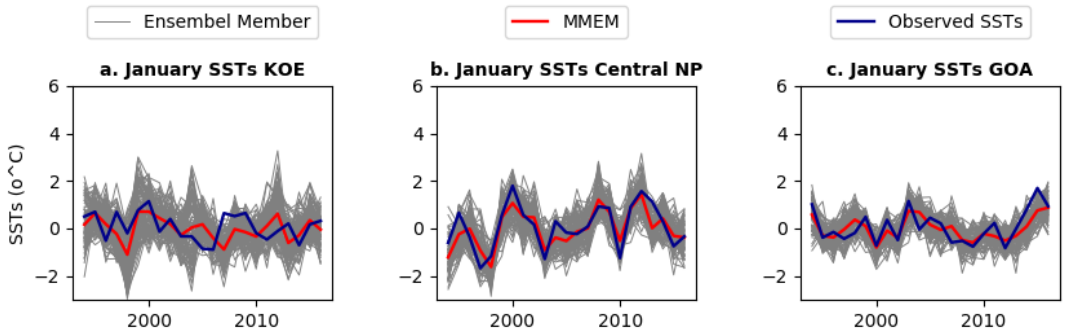

Figure 3.3. Area-averaged time series of MMEM (red), ensemble member (gray) and observed SST anomalies (blue) for the January forecast over (a) the KOE, (b) the Central NP, and (c) the GOA.

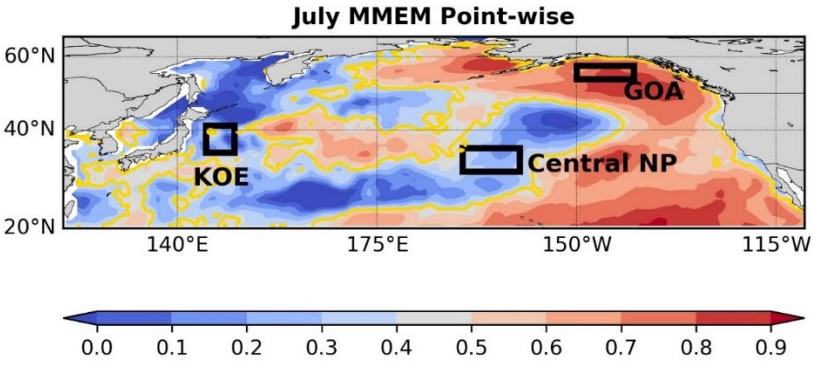

Figure 3.4. Same as in Figure 3.1, but for July forecast.

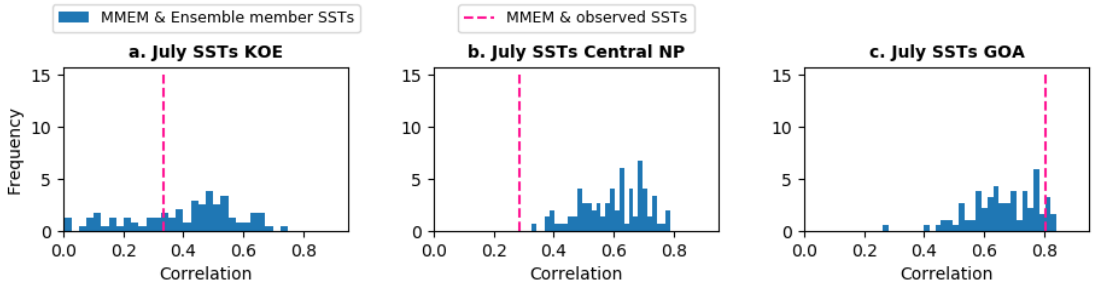

Figure 3.5. Same as in Figure 3.2. but for July forecast.

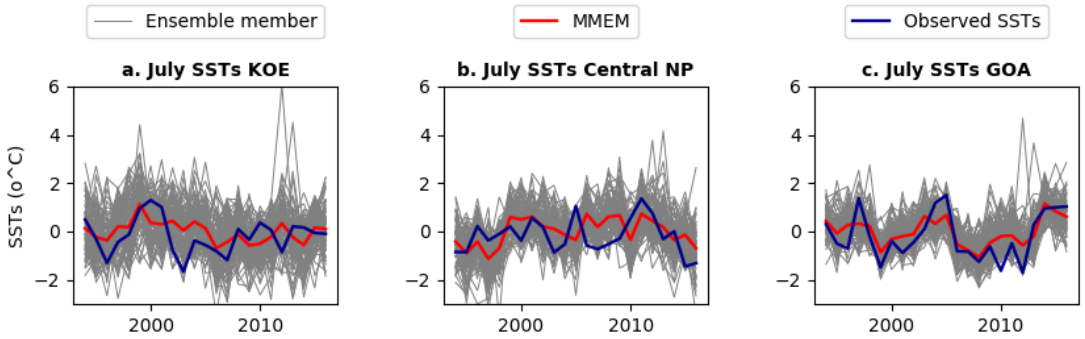

Figure 3.6. Same as in Figure 3.3, but for July forecast.

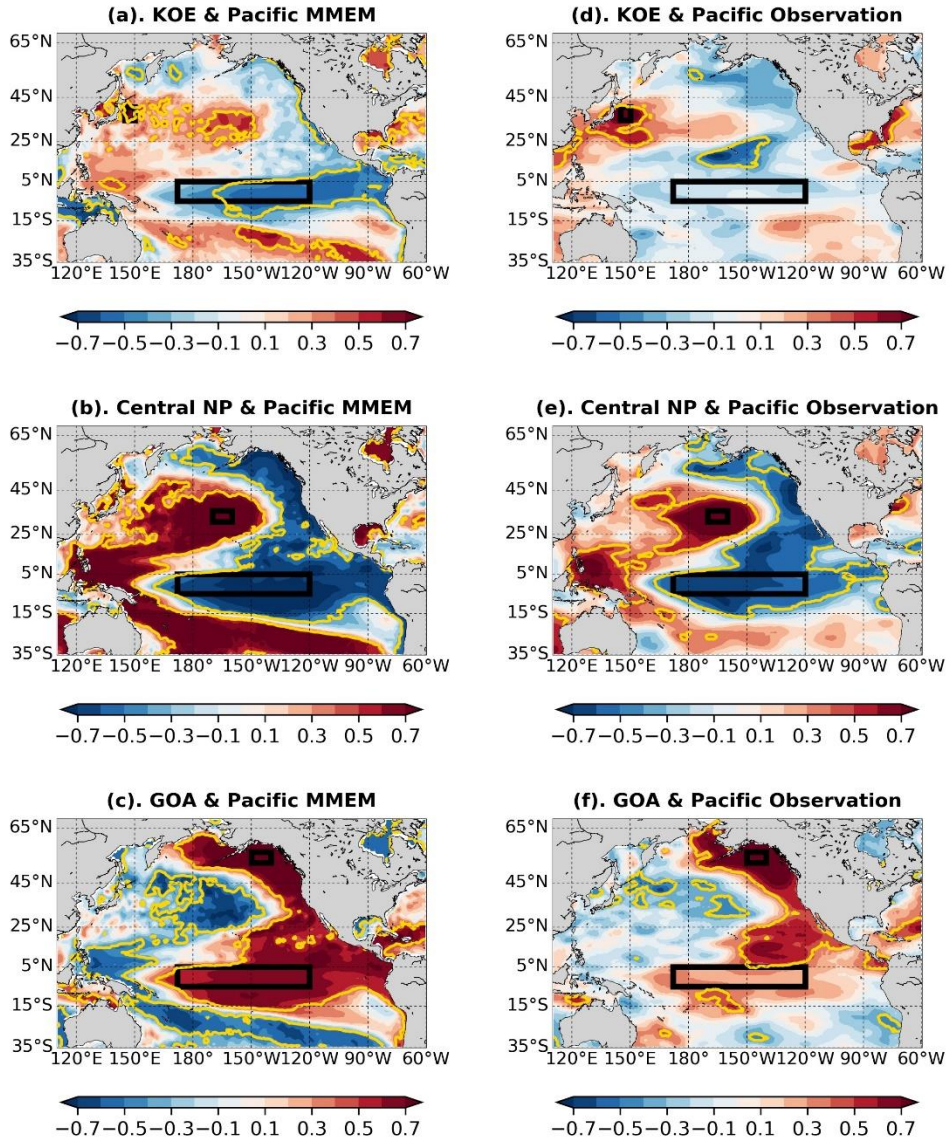

Figure 3.7. (a)-(c) Correlation map between MMEM SSTs time series-averaged over (a) the KOE, (b) the central NP and (c) the GOA and MMEM SSTs each grid points SSTs over the North and tropical Pacific for January. (d)-(f) Same as (a)-(c), but for obsereved SSTs. The black outlines mark the areas of interest and the Niño region. The color shades indicate correlation values and the yellow contours indicate the area where correlations are significant at the 95% confidence level.

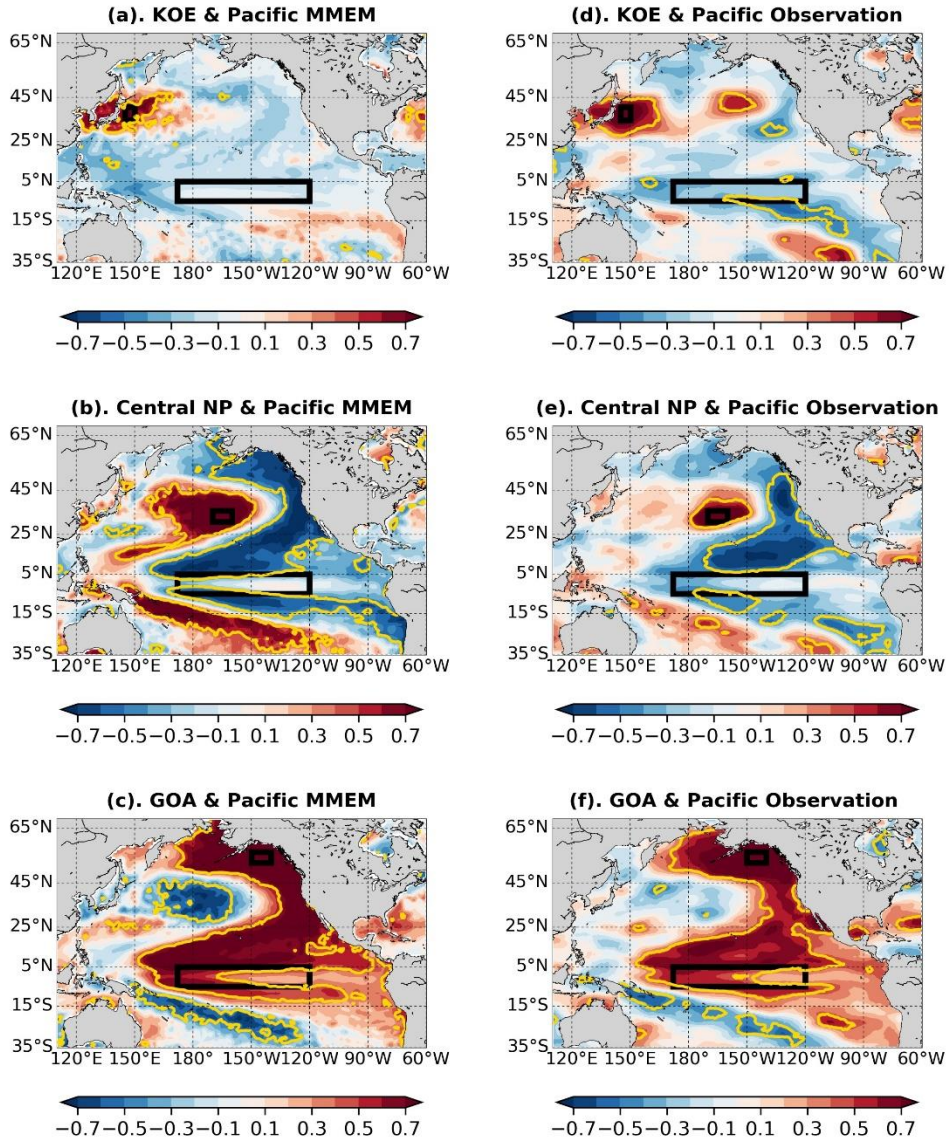

Figure 3.8. Same as in Figure 3.7, but for July.

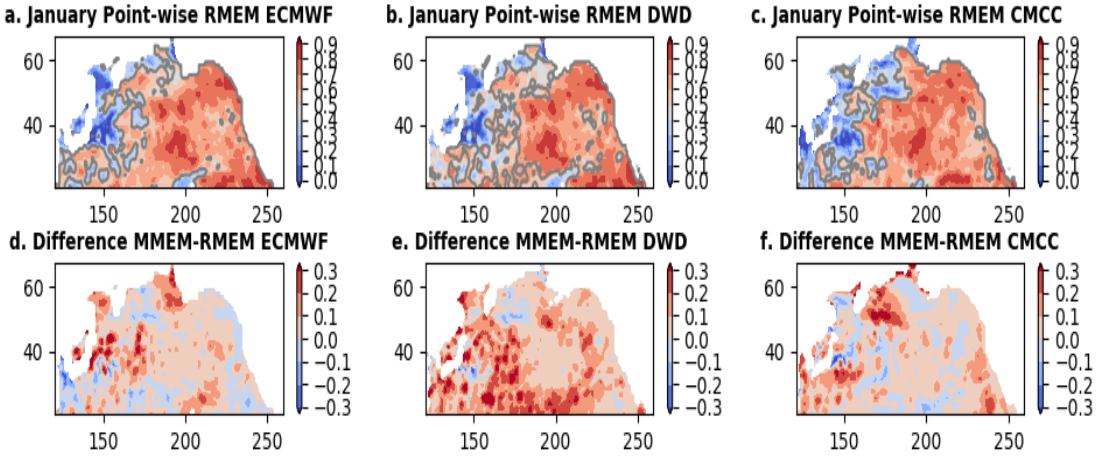

Figure 3.9. Point-wise correlation between RMEM and observed SSTs (top panels) and difference in point-wise correlations between MMEM and RMEM (bottom panels), for ECMWF ((a) and (d)), DWD ((b) and (e)) and CMCC ((c) and (f)), for the January forecast. Contours in panels (a)-(c) indicate the areas where correlations are significant at the 95% confidence level.

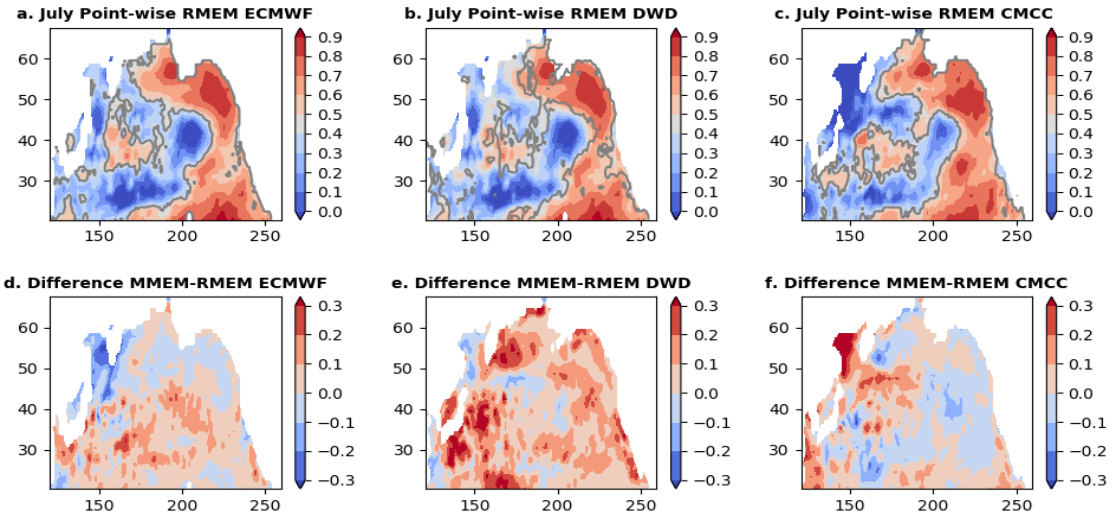

Figure 3.10. Same as in Figure 3.9, but for July forecast.

Chapter 4

General Summary

Marine ecosystem variation and Sea Surface Temperature (SST) predictability in the North Pacific (NP) were investigated in this research. In Chapter 2, marine ecosystem variability in the NP and its relation to large-scale climate variability and change were investigated. In Chapter 3, SST predictability over the NP was evaluated using the latest seasonal forecast systems of the European Centre for Medium-Range Weather Forecasts (ECMWF), Deutscher Wtterdienst (DWD) and Centro-Euro-Mediterraneo Sui Cambiamenti Climatici (CMCC). This chapter summaries major findings from chapter 2 and 3 and discusses implications for future prediction models.

In Chapter 2, the important mode of marine ecosystem variation in the NP and its relation to large scale climate variability and change were identified using large multivariate analysis. An empirical orthogonal function (EOF) was performed on 120 marine biology data to identify the important mode of marine biology and the correlation analysis was applied on important mode of marine biology and physical climate data. The time series of first EOF mode (PC1s) of the marine biology variation for the whole, eastern and western NP were characterized by long-term trends in 1965-2006 corresponding to increases of Alaskan and Japanese/Russian salmon abundance and some Japan small pelagic recruitment and to decreases in groundfish across the basin and in zooplankton in California waters and the Bering Sea. This mode was possibly influenced by global warming. The second EOF mode (PC2) of eastern NP marine ecosystem was characterized by multi-decadal variability related to Pacific Decadal Oscillation (PDO). On the other hand, the western NP PC2 marine ecosystem

was characterized by interdecadal variability related to the North Pacific Gyre Oscillation (NPGO).

In Chapter 3, the SST predictability over the NP in the Multi Model Ensemble Mean (MMEM) from seasonal forecast system and the relation between ensemble members and observed SST were evaluated by correlation analysis. The point-wise correlation reveals that the high SST predictability in MMEM are found in GOA for January and July forecast and central NP for January forecast. On the other hand, the low SST predictability in MMEM are found in the KOE for January and July forecast and in the central NP for July forecast. Further analysis reveals that the high SST predictability in MMEM is related to small ensemble spread and strong predictable components (i.e., MMEM). In contrast, the low SST predictability in MMEM is related to either the large ensemble spread, or due to small ensemble spread but ensemble members cannot capture observations. The small ensemble spread but ensemble members cannot capture observation results from biased variation that is common among ensemble members.

As mentioned in Chapter 1, information about climate and marine ecosystem co-variability as well as seasonal SST predictability from climate forecasting systems can be used for future predictions of marine ecosystem change. However, there was a gap in time scale between Chapter 2 and Chapter 3. In Chapter 2, the correlation between marine ecosystem and climate parameters was mainly due to decadal variability, while in Chapter 3 the multi-model ensemble from the seasonal forecast system can provide SST variation on an interannual time scales. Hence, to know the usefulness of seasonal SST forecast information for prediction of marine ecosystem variations in the North Pacific on interannual time scales, the interannual variability of

marine biology data in Chapter 2 were examined using a high-pass filter. The high-pass filter is calculated by subtracting unfiltered data with low-pass filter data. The low-pass filter data is the filtered data by using 5 years running averaged. The high-pass filter was employed on marine biology and SST data in Chapter 2.

Figure 4.1 shows correlation maps between marine biology PCs and SST in Chapter 2 for 1965-2006 after applying a high-pass filter. Among all principle components (PCs) for the NP marine ecosystem, only the eastern and the whole marine biology PC1 are strongly correlation with SST over the North and topical Pacific on interannual time scales (Figure 4.1.(a) and (c)). Figure 4.1 (a) shows a significant positive correlation between the eastern NP marine ecosystem PC1 and SST around the southern Gulf of Alaska, California water to the tropical Pacific Ocean and a significant negative correlation around southern central NP to western tropical Pacific Ocean. The correlation between the whole NP marine ecosystem PC1 and SST (Figure 4.1.(c)) also showed a similar pattern with eastern NP marine ecosystem PC1. The high-pass filter results indicate that eastern NP marine biology in 1965-2006 was also influenced by SST variability on interannual time scales.

Therefore, to know the future marine ecosystem variability on interannual time scales, it is important to know the future SST variability on interannual time scales. The future SST variability on interannual time scales can be analyzed by using a seasonal forecast system.

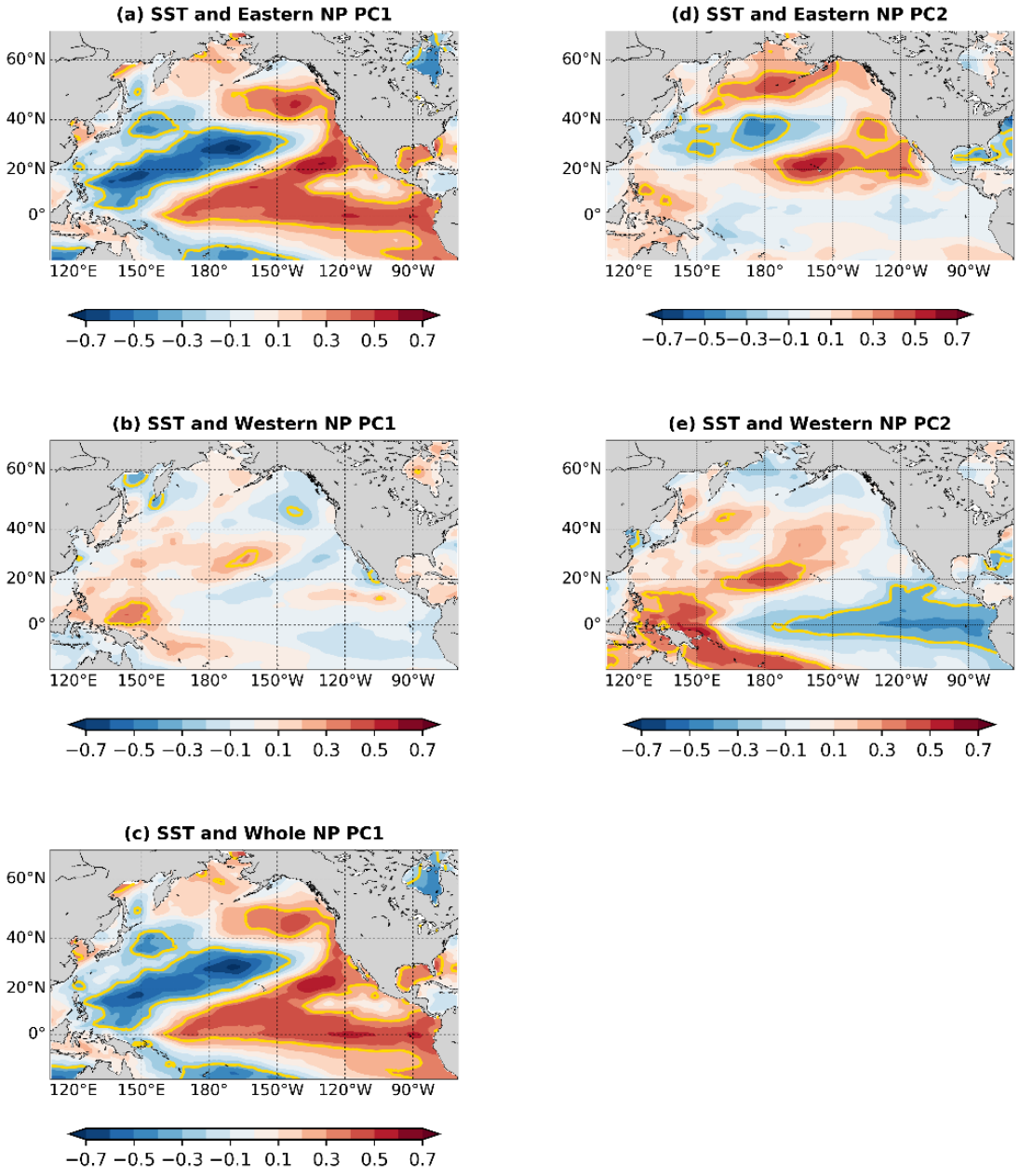

Figure 4.1. Correlation map of SST with (a) eastern NP marine ecosystem PC1, (b) western NP marine ecosystem PC1, (c) whole NP marine ecosystem PC1, (d) eastern NP marine ecosystem PC2 and (e) western NP marine ecosystem PC2, after high-pass filtered, during 1965-2006. The colors indicate correlation value and the yellow contours indicates the 95% confidence level.

Acknowledgements

I would like to express the sincerest gratitude to my academic supervisor Prof. Shoshiro Minobe for teaching me many valuable lessons, offering many useful suggestions, and being there for indispensable discussion and support. Without his support and encouragement, I would not have been able to complete my doctoral studies. I would also like to express my gratitude to Prof. Nathan Mantua and Prof. Shin-ichi Ito for allowing me to use their marine biology data, and for their suggestions and encouragement during my study. I would also like to extend my sincere thanks to Prof. Emanuele Di Lorenzo, Prof. Masaharu Inatsu, Assoc-Prof. Masahiko Fujii, and Assoc-Prof. Yoshinori Sasaki for providing me with constructive comments and suggestions. Finally, I wish to express my heartfelt thanks to Indonesian National Institute Aeronautics and Space (LAPAN) and the Research and Innovation Science and Technology Project, Ministry of Research and Technology/ National Research and Innovation Agency of Republic of Indonesia for funding my doctoral course.

References

Alexander MA, Bladé I, Newman M, Lanzante JR, Lau N-C, Scott JD. 2002. The atmospheric bridge: the influence of ENSO teleconnections on air-sea interaction over the global oceans. J Clim 15:2205–2231.

Allen, M.J. and G.B. Smith, 1988. Atlas and zoogeography of common fishes in the Bering Sea and Northeastern Pacific. NOAA Tech. Rep. NMFS 66: 151.

Beamish, R.J., and Bouillon, D.R. 1993. Pacific Salmon Production Trends in Relation to Climate. Canadian Journal of Fisheries and Aquatic Science 50: 1002–1016. doi:10.1139/f93-116.

Beamish, R.J., Neville, C.-E.M., and Cass, A.J. 1997. Production of Fraser River sockeye salmon (*Oncorhynchus nerka*) in relation to decadal-scale changes in the climate and the ocean. Canadian Journal of Fisheries and Aquatic Science 54: 543-554. doi:10.1139/f96-310.

Beamish, R.J., Noakes, D.J., Mcfarlane, G.A., Klyashtorin, L., Ivanov, V. v, and Kurashov, V. 1999. The regime concept and natural trends in the production of Pacific salmon. Canadian Journal of Fisheries and Aquatic Science 56: 516–526. doi:10.1139/f98-200.

Becker, E., van den Dool, H., and Zhang, Q. 2014. Predictability and forecast skill in NMME. Journal of Climate 27(15): 5891–5906. doi:10.1175/JCLI-D-13-00597.1.

Bindoff, N.L., W.W.L. Cheung, J.G. Kairo, J. Arístegui, V.A. Guinder, R. Hallberg, N. Hilmi, N. 430 Jiao, M.S. Karim, L. Levin, S. O'Donoghue, S.R. Purca Cuicapusa, B. Rinkevich, T. Suga, A. 431 Tagliabue, and P. Williamson, 2019. Changing Ocean, Marine Ecosystems, and Dependent 432 Communities. In: IPCC Special Report on the Ocean and Cryosphere in a Changing Climate 433 [H.-O. Pörtner, D.C. Roberts, V. Masson-Delmotte, P. Zhai, M. Tignor, E. Poloczanska, K. 434 Mintenbeck, A. Alegría, M. Nicolai, A. Okem, J. Petzold, B. Rama, N.M. Weyer (eds.)]. In 435 press.

Bond, N.A., Overland, J.E., Spillane, M., and Stabeno, P. 2003. Recent shifts in the state of the North Pacific. Geophysical Research Letters 30(23). American Geophysical Union. doi:10.1029/2003GL018597.

Borje, J. and N.R. Hareide. 1993.Trial deepwater longline fishery in the Davis Current, May-June. Northwest Atlantic Fisheries Organization, Dartmouth, N.S. 6 p. SCR Doc. 93/53.

Brodeur, Rd, et al. 2002. Increases in Jellyfish Biomass in the Bering Sea: Implications for the Ecosystem. Marine Ecology Progress Series 233: 89–103. doi:10.3354/meps233089.

Carothers, C., Sformo, T.L., Cotton, S., George, J.C., and Westley, P.A.H. 2019. Pacific salmon in the rapidly changing arctic: Exploring local knowledge and emerging fisheries in Utqiaġvik and Nuiqsut, Alaska. Arctic 72(3): 273–288. Arctic Institute of North America. doi:10.14430/arctic68876.

Chavez, F.P., Ryan, J., and Lluch-Cota, S.E. 2003. From Anchovies to Sardines and Back: Multidecadal Change in the Pacific Ocean. Science 299: 217–221. doi:10.1126/science.1075880.

Coad, B. W., and Jim D. Reist. 2004. Annotated List of the Arctic Marine Fishes of Canada. Can. MS Rep. Fish Aquat. Sci. 2674: 112.

Collette, Bruce B., and Cornelia E. Nauen. 1983. FAO Species Catalogue, Vol. 2: Scombrids of the World: An Annotated Catalogue of Tunas, Mackerels, Bonitos and Related Species Known to Date. Food and Agriculture Organization of the United Nations.

Di Lorenzo, E., Schneider, N., Cobb, K.M., Franks, P.J.S., Chhak, K., Miller, A.J., McWilliams, J.C., Bograd, S.J., Arango, H., Curchitser, E., Powell, T.M., and Rivière, P. 2008. North Pacific Gyre Oscillation links ocean climate and ecosystem change. Geophysical Research Letters 35(8). doi:10.1029/2007GL032838.

Di Lorenzo, E., Combes, V., Keister, J.E., Strub, P.T., Thomas, A.C., Franks, P.J.S., Ohman, M.D., Furtado, J.C., Bracco, A., Bograd, S.J., Peterson, W.T., Schwing, F.B., Chiba, S., Taguchi, B., Hormazabal, S., and Parada, C. 2013. Synthesis of Pacific Ocean climate and ecosystem dynamics. Oceanography 26(4): 68–81. doi:10.5670/oceanog.2013.76.

Doi, T., Behera, S.K., and Yamagata, T. 2016. Improved seasonal prediction using the SINTEX-F2 coupled model. Journal of Advances in Modeling Earth Systems 8(4): 1847–1867. Blackwell Publishing Ltd. doi:10.1002/2016MS000744.

Doi, T., S.K. Bahera and Toshio Yamagata. 2019. Merits of a 108-member ensemble system in ENSO and IOD Prediction. Journal of Climate. 32: 957-972. doi: 10.1175/JCLI-D-18-0193.1

Ebbesmeyer, C.C., Cayan, D.R., McLain, D.R., Nichols, F.H., Peterson, D.H., and Redmond, K.T. 1991. 1976 step in the Pacific climate: forty environmental changes between 1968–1975 and 1977–1984. *In* Proceedings of the Seventh Annual Climate (PACLIM) Workshop:115–126.

Eisner, Lisa B., et al. 2014. Climate-Mediated Changes in Zooplankton Community Structure for the Eastern Bering Sea." Deep Sea Research Part II: Topical Studies in Oceanography 109: 157–171. doi:10.1016/j.dsr2.2014.03.004.

Eschmeyer, William N., et al. 1983. A Field Guide to Pacific Coast Fishes of North America: from the Gulf of Alaska to Baja California. Houghton Mifflin: xii+336.

FAO-FIGIS. A world overview of species of interest to fisheries. Chapter: Trachurus japonicus. Retrieved on 12 July 2005, from www.fao.org/figis/servlet/species?fid=2308. 2p. FIGIS Species Fact Sheets. Species Identification and Data Programme-SIDP, FAO-FIGIS.

Fedorov, V.V., I.A. Chereshnev, M.V. Nazarkin, A.V. Shestakov and V.V. Volobuev. 2003. Catalog of marine and freshwater fishes of the northern part of the Sea of Okhotsk. Vladivostok: Dalnauka: 204.

Francis, R.C., and Hare, S.R. 1994. Decadalcscale regime shifts in the large marine ecosystems of the Northleast Pacific: a case for historical science. Fishereis Oceanography 3(4): 279–291. doi:10.1111/j.1365-2419.1994.tb00105.x.

Fricke, R., M. Kulbicki and L. Wantiez. 2011. Checklist of the fishes of New Caledonia, and their distribution in the Southwest Pacific Ocean (Pisces). Stuttgarter Beiträge zur Naturkunde A, Neue Serie 4:341-463.

Froese, R. and D. Pauly. Editors. 2019. FishBase. World Wide Web electronic publication.www.fishbase.org, (access December 19, 2019).

Goericke, R., et al. 2014. CalCoFI & CCE-LTER: 60+ Years of Ocean Observations. Scripps Institution of Oceanography.

Hare, S.R., Mantua, N.J., and Francis, R.C. 1999. Inverse Production Regimes: Alaska and West Coast Pacific Salmon. Fisheries Habitat 24(1): 6–14. doi:10.1577/1548-8446(1999)024<0006:IPR>2.0.CO;2.

Hare, S.R., and Mantua, N.J. 2000. Empirical evidence for North Pacific regime shifts in 1977 and 1989. *In* Progress in Oceanography. 47: 103-145. doi:10.1016/S0079-6611(00)00033-1.

Hart, J.L.1973. Pacific fishes of Canada. Bull. Fish. Res. Board Can. 180:740.

Hirahara, S., Ishii, M., and Fukuda, Y. 2014. Centennial-scale sea surface temperature analysis and its uncertainty. Journal of Climate 27(1): 57–75. doi:10.1175/JCLI-D-12-00837.1.

Hobday, A.J., Spillman, C.M., Eveson, J.P., Hartog, J.R., Zhang, X., and Brodie, S. 2018. A framework for combining seasonal forecasts and climate projections to aid risk management for fisheries and aquaculture. Frontiers in Marine Science 5(APR). Frontiers Media S. A. doi:10.3389/fmars.2018.00137.

Ikeda, Tsutomu, et al. 2008. Structure, Biomass Distribution and Trophodynamics of the Pelagic Ecosystem in the Oyashio Region, Western Subarctic Pacific. Journal of Oceanography 64(3): 339–354. doi:10.1007/s10872-008-0027-z.

Inada, T., 1995. Merlucciidae. Merluzas. In W. Fischer, F. Krupp, W. Schneider, C. Sommer, K.E. Carpenter and V. Niem (eds.) Guia FAO para Identification de Especies para lo Fines de la Pesca. Pacifico Centro-Oriental. 3: 1272-1274. FAO, Rome

Ito, T., Minobe, S., Long, M.C., and Deutsch, C. 2017. Upper ocean O2 trends: 1958–2015. Geophysical Research Letters 44(9): 4214–4223. Blackwell Publishing Ltd. doi:10.1002/2017GL073613.

Ito, T., Long, M.C., Deutsch, C., Minobe, S., and Sun, D. 2019. Mechanisms of Low-Frequency Oxygen Variability in the North Pacific. Global Biogeochemical Cycles 33(2): 110–124. Blackwell Publishing Ltd. doi:10.1029/2018GB005987.

Iwatsuki, Y., M.Akazaki and N. Taniguchi. 2007. Review of the species of the genus Dentex (Perciformes:Sparidae) in the Western Pacific defined as the D. hypselosomus complex with the description of a new species, Dentex abei and a redescription of Evynnis tumifrons. Bull. Natl. Mus. Nat. Sci. Ser. A. Suppl. 1:29-49.

Jacox, M.G., Alexander, M.A., Stock, C.A., and Hervieux, G. 2019. On the skill of seasonal sea surface temperature forecasts in the California Current System and

its connection to ENSO variability. Climate Dynamics 53(12): 7519–7533. Springer Verlag. doi:10.1007/s00382-017-3608-y.

Joh, Y., and Di Lorenzo, E. 2017. Increasing Coupling Between NPGO and PDO Leads to Prolonged Marine Heatwaves in the Northeast Pacific. Geophysical Research Letters 44(22): 11,663-11,671. Blackwell Publishing Ltd. doi:10.1002/2017GL075930.

Johnson, S.J., Stockdale, T.N., Ferranti, L., Balmaseda, M.A., Molteni, F., Magnusson, L., Tietsche, S., Decremer, D., Weisheimer, A., Balsamo, G., Keeley, S.P.E., Mogensen, K., Zuo, H., and Monge-Sanz, B.M. 2019. SEAS5: The new ECMWF seasonal forecast system. Geoscientific Model Development 12(3): 1087–1117. Copernicus GmbH. doi:10.5194/gmd-12-1087-2019.

Kaeriyama, M., Seo, H., and Qin, Y. xue. 2014. Effect of global warming on the life history and population dynamics of Japanese chum salmon. Springer-Verlag Tokyo. doi:10.1007/s12562-013-0693-7.

Kawasaki, T., and Omori, M. 1995. Possible mechanisms underlying fluctuations in the Far Eastern sardine population inferred from time series of two biological traits. Fishereis Oceanography 4(3): 238–242. doi:10.1111/j.1365-2419.1995.tb00147.x.

Kells, Val, et al. 2016.A Field Guide to Coastal Fishes: from Alaska to California. Johns Hopkins University Press.

Kirtman, B.P., et al. 2014. The North American multimodel ensemble: Phase-1 seasonal-to-interannual prediction; phase-2 toward developing intraseasonal prediction. Bulletin of the American Meteorological Society 95(4): 585–601. American Meteorological Society. doi:10.1175/BAMS-D-12-00050.1.

Kramer, D.E. and V.M. O'Connell. 1995. Guide to Northeast Pacific rockfishes. Genera Sebastes and Sebastolobus. Alaska Sea Grant, Marine Advisory Bulletin No. 25.

Li, L., Hollowed, A.B., Cokelet, E.D., Barbeaux, S.J., Bond, N.A., Keller, A.A., King, J.R., McClure, M.M., Palsson, W.A., Stabeno, P.J., and Yang, Q. 2019. Subregional differences in groundfish distributional responses to anomalous ocean bottom temperatures in the northeast Pacific. Global Change Biology 25(8): 2560–2575. Blackwell Publishing Ltd. doi:10.1111/gcb.14676.

Litzow, M.A., and Mueter, F.J. 2014. Assessing the ecological importance of climate regime shifts: An approach from the North Pacific Ocean. Progress in Oceanography 120: 110–119. doi:10.1016/j.pocean.2013.08.003.

Lluch-Belda, D., et al.1989. World-Wide Fluctuations of Sardine and Anchovy Stocks: the Regime Problem. South African Journal of Marine Science 8(1): 195–205., doi:10.2989/02577618909504561.

Lluch-Belda, D., Schwartzlose, R.A., Serra, R., Parrish, R., Kawasakl, T., Hedgecockp, D., M Crawford, R.J., Paz, L., California Sur, B., and of Californiu-San Diego, Zu. 1992. Sardine and anchovy regime fluctuations of abundance in four regions of the world oceans: a workshop report. Fishereis Oceanography 1(4): 339–347. doi: 10.1111/j.1365-2419.1992.tb00006.x.

Love, Milton S., et al. 2002. The Rockfishes of the Northeast Pacific. University of California Press.

Ma, S., Liu, Y., Li, J., Fu, C., Ye, Z., Sun, P., Yu, H., Cheng, J., and Tian, Y. 2019. Climate-induced long-term variations in ecosystem structure and atmosphere-ocean-ecosystem processes in the Yellow Sea and East China Sea. Progress in Oceanography 175: 183–197. Elsevier Ltd. doi:10.1016/j.pocean.2019.04.008.

Mantua, N.J., Hare, S.R., Zhang, Y., Wallace, J.M., and Francis, R.C. 1997. The Pacific Decadal Oscillation. Journal of Oceanography. Bulletin of the American Meteorological Society 78(6): 1069–1079. doi:10.1175/1520-0477(1997)078<1069:APICOW>2.0.CO;2.

Min, Y.M., Ham, S., Yoo, J.H., and Han, S.H. 2020. Recent progress and future prospects of subseasonal and seasonal climate predictions. *In* Bulletin of the American Meteorological Society. American Meteorological Society: E640–E644. doi:10.1175/BAMS-D-19-0300.1.

Minobe, S. 1997. A 50-70 year climatic oscillation over the North Pacific and North America. Geophysical Research Letters 24(6): 683–686. American Geophysical Union. doi:10.1029/97GL00504.

Minobe, S. 2000. Spatio-temporal structure of the pentadecadal variability over the North Pacific. *In* Progress in Oceanography 47(2-4):381-408. doi:10.1016/s0079-6611(00)00042-2.

Möllmann, C., and Diekmann, R. 2012. Marine Ecosystem Regime Shifts Induced by Climate and Overfishing. A Review for the Northern Hemisphere. *In* Advances in Ecological Research. Academic Press Inc: 303–347. doi:10.1016/B978-0-12-398315-2.00004-1.

Muus, Bent J., et al. 1999. Sea Fish. Scandinavian Fishing Yearbook.

Nakabo, Tetsuji. 2002. Fishes of Japan: with Pictorial Keys to the Species: English Edition. Tokai University Press.

Nakanowatari, T., Ohshima, K.I., and Wakatsuchi, M. 2007. Warming and oxygen decrease of intermediate water in the northwestern North Pacific, originating from the Sea of Okhotsk, 1955-2004. Geophysical Research Letters 34(4). doi:10.1029/2006GL028243.

Noto, M., and Yasuda, I. 1999. Population decline of the Japanese sardine, Sardinops melanostictus, in relation to sea surface temperature in the Kuroshio Extension. Canadian Journal of Fisheries and Aquatic Science 56(6): 973–983. doi:10.1139/f99-028.

Ono, T., Midorikawa, T., Watanabe, Y.W., Tadokoro, K., and Saino, T. 2011. Temporal increases of phosphate and apparent oxygen utilization in the subsurface water of western subarctic Pacific from 1968 to 1998. Geophysical Research Letters 28(17): 3285–3288. doi:10.1029/2001GL012948.

Orr, J.W. and J.E. Blackburn. 2004. The dusky rockfishes (Teleostei: Scorpaeniformes) of the North Pacific Ocean: resurrection of Sebastes variabilis (Pallas, 1814) and a redescription of Sebastes ciliatus (Tilesius, 1813). Fish. Bull. 102:328-348.

Ou, W., Haigh, R., Ackerman, B., Tadey, R., Li, M., and Robinson, C. 2012. Rougheye and blackspotted rockfish complex and longspine thorny management plan. https://www.canada.ca/en/environment-climate-change/services/species-risk-public-registry/management-plans/rougheye-rockfish-complex-longspine-thornyhead-2012.html (access on December 9, 2019).

Pinsky, M.L., Worm, B., Fogarty, M.J., Sarmiento, J.L., and Levin, S.A. 2013. Marine Taxa Track Local Climate Velocities. Science 341(6151): 1236–1239. American Association for the Advancement of Science. doi:10.1126/science.1239373.

Poloczanska, E.S., Burrows, M.T., Brown, C.J., Molinos, J.G., Halpern, B.S., Hoegh-Guldberg, O., Kappel, C. v., Moore, P.J., Richardson, A.J., Schoeman, D.S., and

Sydeman, W.J. 2016. Responses of marine organisms to climate change across oceans. Frontiers in Marine Science 3. doi:10.3389/fmars.2016.00062.

Pozo Buil, M., and Di Lorenzo, E. 2017. Decadal dynamics and predictability of oxygen and subsurface tracers in the California Current System. Geophysical Research Letters 44(9): 4204–4213. Blackwell Publishing Ltd. doi:10.1002/2017GL072931.

Riede, Klaus. 2004. Global Register of Migratory Species: from Global to Regional Scales: Final Report of the R & D-Projekt 808 05 081. Federal Agency for Nature Conservation.

Russian Academy of Sciences. 2000. Catalog of vertebrates of Kamchatka and adjacent waters. Kamchatsky Pechatny Dvor, Petropavlovsk-Kamchatsky, Russia: 166.

Samaniego, et al. 2019. Hydrological forecat and projection for improved decision-making in the water sector in Europe. Bull Am Meteorol Soc: 2451-2453.

Stevens, Bradley Gene. 2014. King Crabs of the World: Biology and Fisheries Management. CRC Press.

Sumaila, U.R., Cheung, W.W.L., Lam, V.W.Y., Pauly, D., and Herrick, S. 2011, December. Climate change impacts on the biophysics and economics of world fisheries. Nat. Clim Change 1: 449-456. doi:10.1038/nclimate1301.

Thompson, D.W.J., and Wallace, J.M. 1998. The Arctic oscillation signature in the wintertime geopotential height and temperature fields. Geophysical Research Letters 25(9): 1297–1300. American Geophysical Union. doi:10.1029/98GL00950.

Tian, Y., Kidokoro, H., and Watanabe, T. 2006. Long-term changes in the fish community structure from the Tsushima warm current region of the Japan/East Sea with an emphasis on the impacts of fishing and climate regime shift over the last four decades. Progress in Oceanography 68(2–4): 217–237. doi:10.1016/j.pocean.2006.02.009.

Tobor, J.G. 1972. The food and feeding habits of some Lake Chad commercial fishes. Bull. I.F.A.N. (A) 34(1): 179-211.

Tommasi, D., et al. 2017. Managing living marine resources in a dynamic environment: The role of seasonal to decadal climate forecasts. Progress in Oceanography 152: 15-49. doi:10.1016/j.pocean.2016.12.011.

Trenberth, K.E., and Hurrell, J.W. 1994. Decadal atmosphere-ocean variations in the Pacific. Climate Dynamics 9: 303–319. doi:10.1007/BF00204745.

von Storch, Hans Von, and Francis Zwiers. 2012. Testing Ensembles of Climate Change Scenarios for 542 Statistical Significance. Climatic Change 117(1-2): 1–9. doi:10.1007/s10584-012-0551-0

Wanders, et al. 2019. Development and evaluation of a Pan-Europian multimodel seasonal hydrological forecasting system. Journal of Hydrometeorology. 20: 99-115. DOI: 10.1175/JHM-D-18-0040.1.

Whitehead, Peter J. P. 1985. FAO Species Catalogue. United Nations Development Programme, Food and Agriculture Organization of the United Nations.

Wolter, K., and Timlin, M.S. 2011. El Niño/Southern Oscillation behaviour since 1871 as diagnosed in an extended multivariate ENSO index (MEI.ext). International Journal of Climatology 31(7): 1074–1087. doi:10.1002/joc.2336.

Yamada, U., S. Shirai, T. Irie, M. Tokimura, S. Deng, Y. Zheng, C. Li, Y.U. Kim and Y.S. Kim. 1995. Names and illustrations of fishes from the East China Sea and the Yellow Sea: 288. Overseas Fishery Cooperation Foundation, Tokyo, Japan.

Yasuda, I., Sugisaki, H., Watanabe, Y., Minobe, S.-S., and Oozeki, Y. 1999. Interdecadal variations in Japanese sardine and ocean/climate. Fisheries Oceanography 8(1): 18–24. doi:10.1046/j.1365-2419.1999.00089.x.

Yasunaka, S., and Hanawa, K. 2002. Regime Shifts Found in the Northern Hemisphere SST Field. Journal of the Meterorological Society of Japan 80(1): 199-135. doi:10.2151/jmsj.80.119.